



**KTH Industrial Engineering  
and Management**

Department of Energy Technology

# Receiver Design Methodology for Solar Tower Power Plants

*Master Thesis*

**Joseph Stalin**

Supervisors:

Dipl.-Ing. Peter Schöttl, Internal Supervisor, Fraunhofer ISE, Freiburg

Dr. Björn Laumert, External Supervisor, KTH Royal Institute of Technology

KTH School of Industrial Engineering and Management  
Department of Energy Technology  
Division of Heat and Power Technology  
SE - 100 44, Stockholm  
July 2016

# Abstract

Among other concentrated solar power (CSP) technologies, solar tower power plants are gaining momentum because of its higher concentration and high potential to reduce costs by means of increasing the capacity factor of the plant with storage. In solar tower power plants (CRS), sunlight is focused onto the receiver by the arrangement of thousands of mirrors to convert it into heat to drive thermal cycles. Solar receivers are used to transfer the flux from the solar field to the working fluid. Generally, solar receivers work in a high-temperature environment and so they are subjected to different heat losses. Also, the receiver plays an important role while accounting for the total cost of the power plant. Thus, the design and modelling of the receiver have a significant influence on the efficiency and the cost of the plant. The goal of the master thesis is to develop a design methodology to calculate the geometry of the receiver and its efficiency. The design methodology is mainly aimed at large-scale power plants in the range of 100 MWe, but also the scalability of the design method will be studied. Then, the developed receiver design method will be implemented in the in-house design tool *devISE<sub>crs</sub>* and will also be integrated with the other modules like solar-field, storage and power-block to calculate the overall efficiency of the power plant. The design models for the other components are partly already implemented, but will be modified and/or extended according to the requirements of CRS plants. Finally, the entire receiver design model is validated by comparing the results of test cases with the data from the literature.

# Contents

<b>Contents</b>	<b>iii</b>
<b>List of Figures</b>	<b>v</b>
<b>List of Tables</b>	<b>vi</b>
<b>1 Introduction</b>	<b>1</b>
1.1 Solar Radiation . . . . .	1
1.2 Concentrated Solar Power (CSP) . . . . .	2
1.3 Central Receiver Systems (CRS) . . . . .	4
1.4 Research Statement . . . . .	6
1.5 Thesis Overview . . . . .	6
<b>2 Literature Review</b>	<b>7</b>
2.1 Tubular Receivers . . . . .	7
2.1.1 Water/Steam . . . . .	7
2.1.2 Molten Salt . . . . .	8
2.1.3 Liquid Sodium . . . . .	8
2.1.4 Sodium/Salt Binary . . . . .	9
2.2 Receiver Design Methodology . . . . .	10
2.2.1 Falcone [1986] [18] . . . . .	10
2.2.2 Zavoico [2001] [45] . . . . .	10
2.2.3 Lata [2008] [26] . . . . .	10
2.2.4 System Advisory Model (SAM) [43] . . . . .	11
2.3 Design Criteria . . . . .	11
2.3.1 Allowable Peak Flux Limit . . . . .	11
2.3.2 Receiver Sizing . . . . .	12
2.3.3 Receiver Aspect Ratio . . . . .	13
2.3.4 Tube Diameter Selection . . . . .	13
2.3.5 Fluid Flow Path Selection . . . . .	13
2.3.6 Tower Sizing . . . . .	14
2.4 Cavity Specific Design Criteria . . . . .	15
2.4.1 Cavity Receiver Geometry . . . . .	15
2.4.2 Cavity Opening Angle . . . . .	16
2.4.3 Lip Height (Aperture to Total Height Ratio) . . . . .	16
2.4.4 Cavity Inclination . . . . .	16
2.5 Heat Transfer Model . . . . .	16
2.5.1 External Receiver . . . . .	16
2.5.2 Cavity Receiver . . . . .	20

---

## CONTENTS

---

<b>3 Design Methodology</b>	<b>23</b>
3.1 Design Approach . . . . .	23
3.2 General Receiver Design Model . . . . .	25
3.2.1 Receiver Thermal Power . . . . .	25
3.2.2 Calculation of HTF Properties . . . . .	25
3.2.3 Receiver Sizing . . . . .	25
3.2.4 Receiver Surface Temperature Calculation . . . . .	26
3.2.5 Mass Flow Rate Calculation . . . . .	27
3.2.6 Pressure Loss and Pump Power Calculation . . . . .	27
3.3 External Receiver Design Model . . . . .	28
3.3.1 Geometry Design . . . . .	28
3.3.2 Tube and Panel Design . . . . .	29
3.3.3 Tower Height Design . . . . .	29
3.3.4 Receiver Thermal Efficiency . . . . .	30
3.4 Cavity Receiver Design Model . . . . .	32
3.4.1 Geometry Design . . . . .	32
3.4.2 Tube and Panel Design . . . . .	34
3.4.3 Tower Height Design . . . . .	34
3.4.4 Receiver Thermal Efficiency . . . . .	34
<b>4 Implementation of the Design Method</b>	<b>37</b>
4.1 Software Description . . . . .	37
4.2 <i>devISE<sub>crs</sub></i> - A Design Tool . . . . .	38
4.3 Implementation Structure of Receiver Module in <i>devISEcrs</i> . . . . .	38
4.4 Inputs/outputs of Receiver Module . . . . .	40
4.4.1 Receiver class . . . . .	40
4.4.2 External receiver class . . . . .	41
4.4.3 Cavity receiver class . . . . .	42
<b>5 Results and Validation</b>	<b>44</b>
5.1 Validation of the Design Method . . . . .	44
5.1.1 External receiver . . . . .	44
5.1.2 Cavity receiver . . . . .	44
5.2 Effect of Spillage Loss on Heliostat Size . . . . .	45
<b>6 Conclusions</b>	<b>46</b>
<b>Bibliography</b>	<b>47</b>

# List of Figures

1.1	Direct radiation vs diffuse radiation [6] . . . . .	1
1.2	World solar DNI map [42] . . . . .	2
1.3	Types of CSP collectors [4] . . . . .	3
1.4	Gemasolar 20MW solar tower power plant in Sevilla, Spain [5] . . . . .	4
1.5	Optical losses in the heliostat field . . . . .	5
1.6	Solar receiver [7] . . . . .	5
2.1	Tubular receivers [43] . . . . .	7
2.2	Flow layout of water/steam central receiver system [2] . . . . .	8
2.3	Flow layout of molten salt central receiver system [43] . . . . .	8
2.4	Flow layout of liquid sodium central receiver system [18] . . . . .	9
2.5	Flow layout of sodium/salt binary central receiver system [18] . . . . .	9
2.6	Receiver peak flux value for different HTF and materials with respect to life cycles [18] . . . . .	12
2.7	Eight possible fluid flow configuration by Wagner [43] . . . . .	14
2.8	Solar tower for external and cavity receivers [19] . . . . .	15
2.9	Cavity receiver with three of four receiver panels assembled in PS10 power plant [19]	15
2.10	Cavity inclination angle [29] . . . . .	16
2.11	Variation of Richardson number with respect to wind velocity for cavity receiver [40]	20
2.12	Two convection zones of the cavity receiver [21] . . . . .	21
3.1	Receiver design methodology for tubular receivers . . . . .	24
3.2	Variation of tower height with respect to receiver thermal power [18] . . . . .	30
3.3	Geometry of cavity receiver [19] . . . . .	33
3.4	Internal angle geometry of cavity receiver [19] . . . . .	33
3.5	Internal heat transfer area of the cavity receiver [36] . . . . .	35
4.1	General structure of the in-house solar tower power plant design and simulation software . . . . .	37
4.2	Modules of the devISEcrs design tool . . . . .	38
4.3	Class inheritance structure of the receiver module in devISEcrs . . . . .	39

# List of Tables

2.1	Receiver flux limit for different HTF [18] . . . . .	11
2.2	Nusselt correlation for forced convection of external receivers [36] . . . . .	19
3.1	Properties of solar salt [45] . . . . .	25
4.1	Input parameters and its default value of the receiver class . . . . .	40
4.2	Input parameters and its default value of the external receiver class . . . . .	41
4.3	Output parameters of the external receiver class . . . . .	41
4.4	Input parameters and its default value of the cavity receiver class . . . . .	42
4.5	Output parameters of the cavity receiver class . . . . .	43
5.1	Gemasolar power plant characteristics . . . . .	45
5.2	Comparison of Gemasolar receiver design parameters . . . . .	45

# Nomenclature

## Abbreviations

CRS	Central receiver systems
CSP	Concentrated solar power
DNI	Direct normal irradiance
HTF	Heat transfer fluid

## Greek symbols

$\alpha$	Absorptance	-
$\beta$	Volumetric expansion coefficient	1/K
$\delta$	Thermal expansion coefficient	1/m K
$\epsilon$	Emissivity	-
$\eta$	Efficiency	-
$\mu$	Dynamic viscosity	kg/ms
$\nu$	Kinematic viscosity	m <sup>2</sup> /s
$\rho$	Density	kg/m <sup>3</sup>
$\sigma$	Stefan-Boltzmann constant	W/m <sup>2</sup> K <sup>4</sup>
$\theta$	Cavity opening angle	-
$\nu$	Poisson's ratio	-
$\varepsilon$	Allowable strain of the material	-

## Symbols

$\Delta P$	Pressure difference	N/m <sup>2</sup>
$\dot{m}$	Mass flow rate	kg/s
$\dot{Q}$	Heat energy	KW
$c_p$	Specific heat	J/kgK
$K_s$	Surface roughness	-
$u_{wind}$	Wind velocity	m/s
A	Area	m <sup>2</sup>

---

***LIST OF TABLES***

---

D	Diameter	m
d	Diameter of the receiver tube	m
f	Darcy friction factor	-
g	Acceleration due to gravity	$m/s^2$
Gr	Grashof number	-
H	Height	m
h	Heat transfer coefficient	$W/m^2 K$
k	Thermal conductivity	$W/m K$
L	Length	m
n	Count	-
Nu	Nusselt number	-
P	Power	W
Pr	Prandtl number	-
$q_o$	Allowable peak flux	$W/m^2$
R	Thermal Resistance	$K/W$
r	Radius	m
Ra	Rayleigh number	-
Re	Reynolds number	-
Ri	Richardson number	-
SM	Solar multiple	-
T	Temperature	K
v	Velocity	$m/s$
W	Power	W

**Subscripts**

abs	Absorber
amb	Ambient
ave	Average
c	Characteristic
cond	Conduction
conv	Convection
eff	Effective
el	Electric
env	Envelope

f	Film
for	Forced
htf	Heat transfer fluid
i	Inner
inc	Incident
mix	Mixed
nat	Natural
net	Net
o	Outer
pb	Power block
rad	Radiation
rec	Receiver
ref	Reflection
s	Surface
th	Thermal
tot	Total
tower	Solar tower
tube	Receiver tube
w	Wall

# Chapter 1

## Introduction

The growing energy demand and the environmental pollution urge us to focus on the sustainable power generation. In order to meet the increasing energy demand in a sustainable way, the solar energy has the potential to act as a future energy source. The disappointing issue with solar energy is that it is a variable source of energy. But, the concentrated solar power coupled with storage technology assures dispatchability of the energy. Hence, CSP can act as a promising alternative source of energy in the future. This chapter explains the basic concepts of CSP technology, the research statement and the overview of the thesis.

### 1.1 Solar Radiation

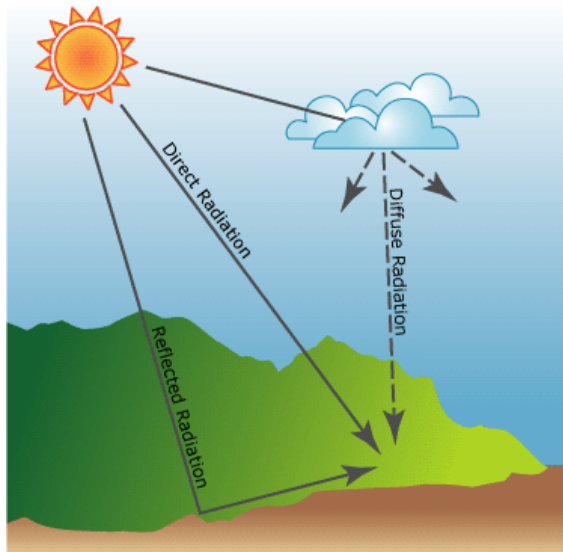


Figure 1.1: Direct radiation vs diffuse radiation [6]

Solar irradiance is the rate of radiant energy per unit area over a period of time produced from the sun. It is usually expressed in Watt per square meter ( $W/m^2$ ) [37]. It can also be said in terms of suns. One sun is equal to  $1000 W/m^2$ . Solar radiation undergoes reflection, absorption and transmission in the earth atmosphere before reaching the ground. This is mainly due to the dust particles in the atmosphere. It determines the amount of sun rays reflected, absorbed and transmitted to the ground. There are mainly two types of radiation based on the reflection and scattering of sun rays. They are

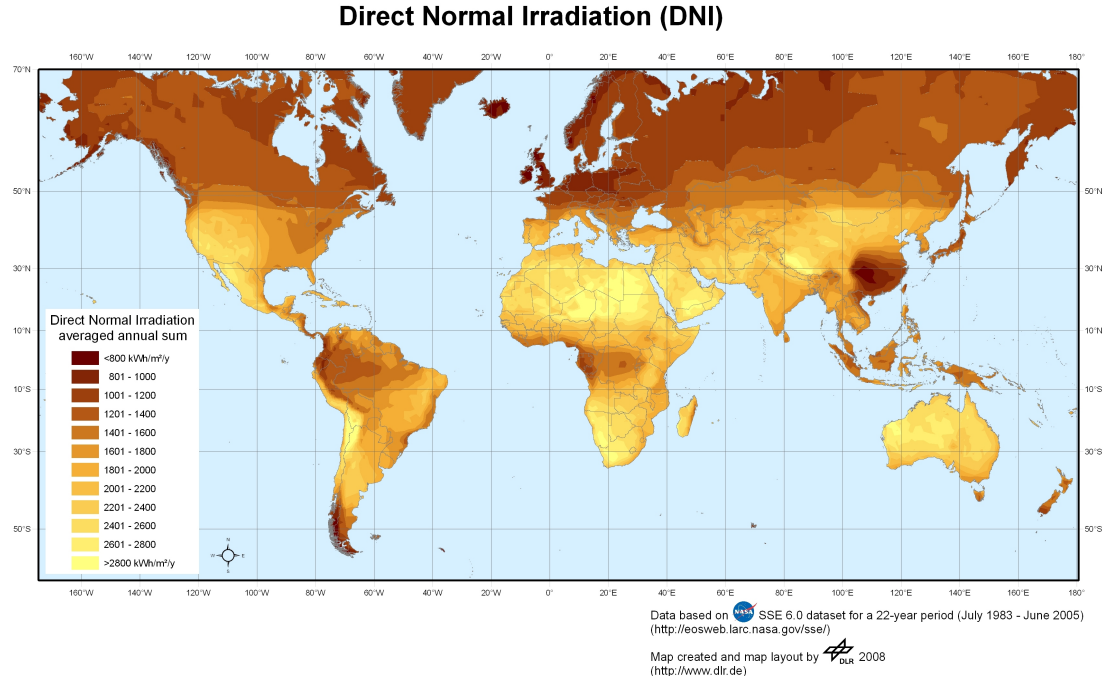


Figure 1.2: World solar DNI map [42]

- Direct radiation
- Diffuse radiation

The part which directly reaches the earth surface without getting scattered by the atmosphere is called direct radiation. Diffuse radiation is the result of scattering by the molecules in the atmosphere and reaching the earth surface. Generally, it is defined as the rate at which the scattered radiant energy falls on a unit horizontal surface per second. Figure 1.1 shows the difference between direct and diffuse radiation.

Solar power plants convert only direct normal irradiance (DNI) into electrical energy [11] and so it is necessary to measure DNI of the site. It is usual to denote DNI as Watt-hour per square meter ( $Wh/m^2$ ) and Watt-hour per square meter per day ( $Wh/m^2/day$ ) for the duration of sunshine hours . The minimum threshold DNI necessary for the solar thermal power plant technology is  $2000\ KWh/m^2/year$  because of economic constraints [11]. In order to have an idea about DNI, world solar DNI map is shown in the Figure 1.2.

## 1.2 Concentrated Solar Power (CSP)

Concentrated solar power (CSP) technology mainly works on the principle of concentrating vast area direct solar insolation onto absorber to convert it into thermal energy. The concentration is done by the perfect reflectors such as mirrors or lenses. Absorbers are used to transfer the obtained solar thermal energy to the heat transfer fluid (HTF). Then, the thermal energy in the HTF is used to generate steam and the electricity is produced by the conventional power cycle. Solar resource is a variable source of energy which cannot be controlled and so it is advisable to incorporate storage into the system. Thus, CSP technology mainly consists of four subsystems [8]:

- Solar collector/field
- Solar receiver
- Storage system
- Power conversion system

Solar collector mainly differs with the shape of collector surface like paraboloid or parabolic trough. It can be summarized in line focusing systems like parabolic trough or linear fresnel collectors and point focusing systems like dish collectors and power towers. These four are the main types of the CSP power plant [8]. Point focusing systems have higher concentration ratio compared to the line focusing systems and so higher temperatures can be easily achieved by point focusing systems [8]. Figure 1.3 clearly gives the overview of the types of CSP power plant. Solar receivers are the

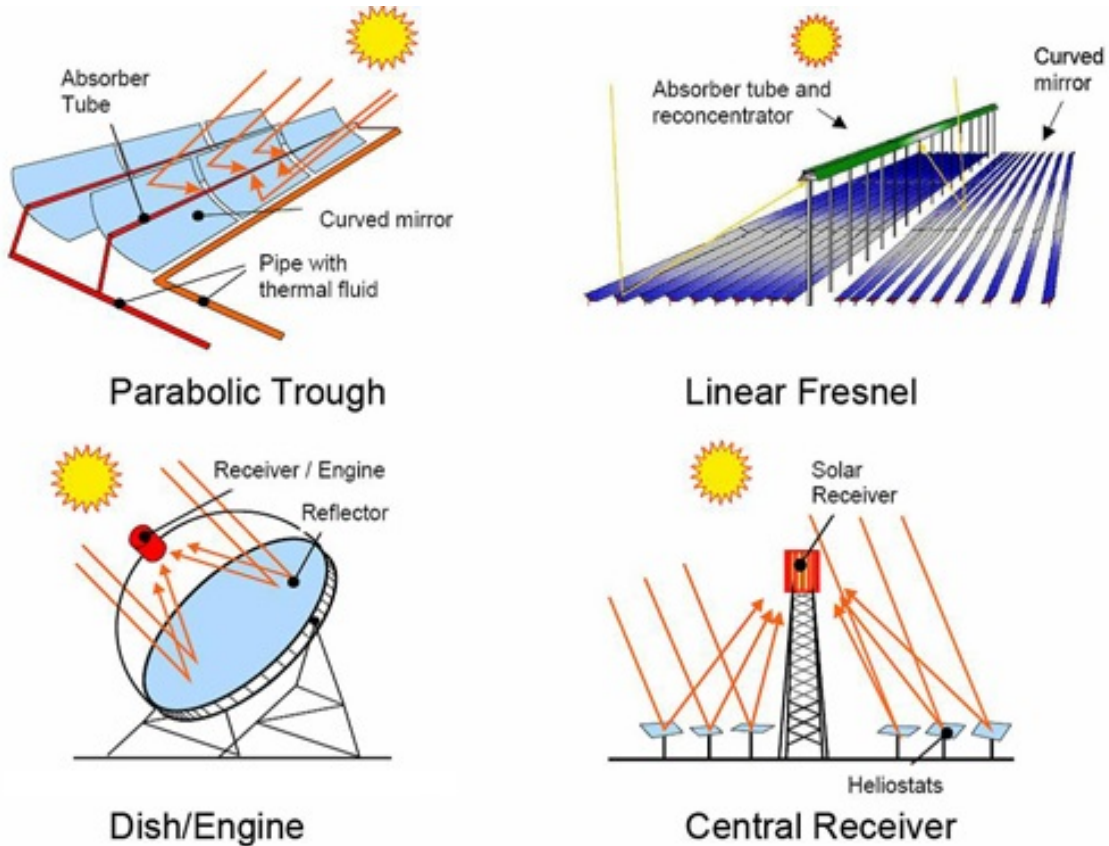


Figure 1.3: Types of CSP collectors [4]

main focus of the thesis and so it is discussed in the separate section. The storage system includes two main categories such as sensible and latent heat storage system. The following are some of the different types of storage system:

- Storage systems
  - Two-tank direct
  - Two-tank indirect
  - Single-tank thermocline
- Storage media

- Concrete
- Phase change materials

Among various types, two-tank molten salt HTF is widely used as a storage technology in CSP plants [13] due to its attractive features like economically cheap [24] and well-established HTF with large-scale industrial experience for many years [22]. The power conversion system is the conventional Rankine, Brayton or combined cycle consisting of turbine, generator, and condenser.

### 1.3 Central Receiver Systems (CRS)

Solar tower power plants are in the class of central receiver systems which have thousands of mirrors (called as heliostats) concentrating solar radiation onto the receiver which is placed on top of the tower at the focal point of heliostats as shown in Figure 1.4. As like other CSP plants, CRS plants also have same four subsystems which are:

- Heliostat field
- Solar receiver
- Storage system
- Power conversion unit

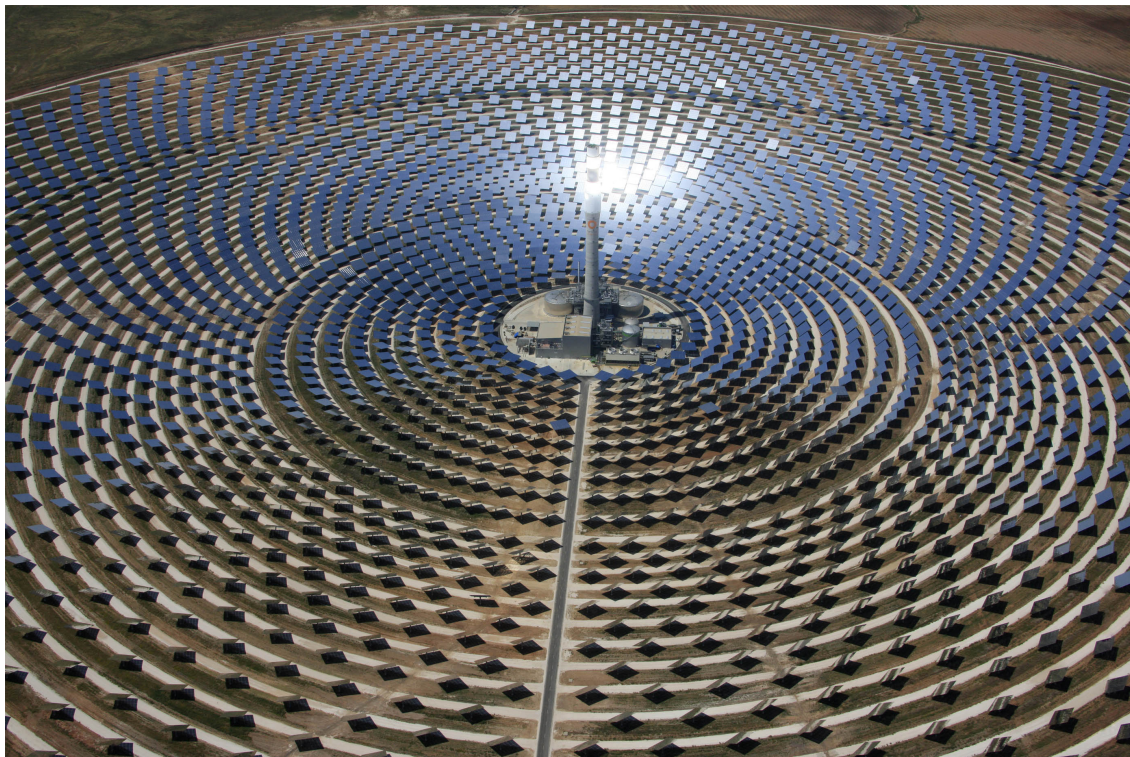


Figure 1.4: Gemasolar 20MW solar tower power plant in Sevilla, Spain [5]

The heliostat field consists of an array of two-axis tracking mirrors which always focuses the radiation at the aim point irrespective of the sun's position. So, the incidence angle of the sun rays varies for every heliostat with respect to the sun's position. At times, when the sun rays are normal to the heliostat, it works effectively. So, the energy lost in terms of change in incidence angle is called cosine loss.

Solar radiation undergoes various optical losses before it reaches the receiver. Figure 1.5 depicts various optical losses in the heliostat field. As the name indicates, shadowing loss is due to shadow caused by the neighbouring heliostats. If the reflected radiation from one heliostat is blocked by the other heliostat, then it is called blocking loss. Because of the dust particles in the path of the radiation to the receiver, attenuation loss occurs. Reflected radiation from the heliostat which can't be able to hit the receiver is called spillage loss. Therefore, the heliostat field should be designed which accounts for low optical losses. Radial staggered pattern is the most widely used layout for designing solar field for CRS plants [35] [33]. The main types of CRS

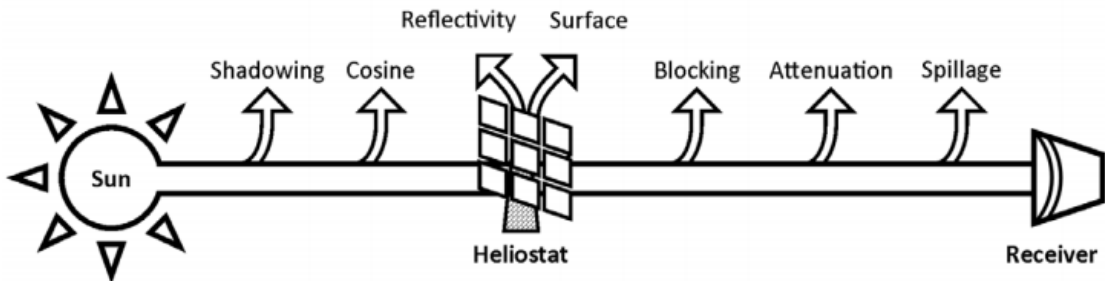


Figure 1.5: Optical losses in the heliostat field

receivers are listed below:

- Tubular receivers
  - External receiver
  - Cavity receiver
- Volumetric receivers
  - Open volumetric air receiver
  - Pressurized air receiver
- Solid particle receivers

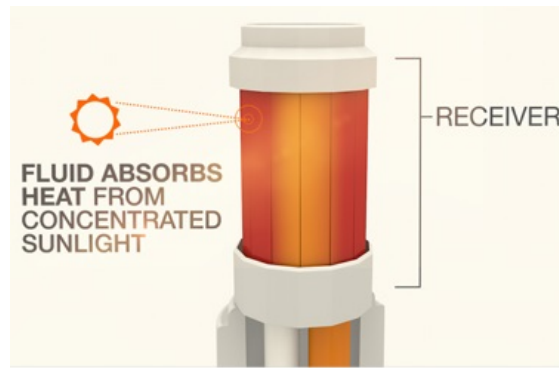


Figure 1.6: Solar receiver [7]

Tubular receivers are the most widely used receiver technology [23] and so the design methodology is limited to only tubular receivers in this study. In tubular receivers, external and cavity are the two most commonly used receivers in CRS plants. The type of receiver directly affects the shape of the solar field. For instance, external receivers will lead to surround type of solar field. But,

the cavity receivers tend to produce the north field for the northern hemisphere and south field for the southern hemisphere.

In external receivers, the absorber tubes are welded to form cylinder-like shape and all the surfaces are exposed to the field. But in cavity receivers, absorber tubes are enclosed in the cavity and there is aperture opening available for the concentrated radiation to hit the absorber.

In PS10, the cavity opening angle for cavity receiver is 180 degrees and so it looks like a half cylinder [19]. It can also be possible to increase the cavity opening angle and multiple cavities can be formed to cover the radiation from the solar field [37]. Due to the enclosed cavity, cavity receiver will have low thermal losses. But, the spillage loss is high compared to external receivers because the entry of concentrated radiation is restricted to the aperture opening. In this study, the design methodology for both types of receivers are developed and it will be implemented in python to create a tool chain which can be used to calculate the geometry, heat losses and the thermal efficiency of the receiver.

## **1.4 Research Statement**

Solar receivers cost around 10 - 15 percent of the total capital investment cost of a power plant [31]. Plant performance, capital cost and the cost of energy produced are significantly affected by the receiver efficiency [36]. Therefore, it is essential to design the receiver carefully in order to increase the plant performance and to minimise the energy cost. In the CRS plants, receivers are the crucial part to design because it should be capable of withstanding high working temperatures, molten salt corrosion and the solar flux transients that cause thermal stress and creep failure [31]. In the recent years, there are several kinds of research going on towards receiver design and optimization and to increase the receiver thermal efficiency [26] [44] [27] [34] [20]. Hence, the main focus of this thesis is on the design of solar receivers.

This research focuses on developing the design methodology for solar central receivers which includes external and cavity receivers. The main objective is to implement the developed design method in the Fraunhofer in-house design tool *devISE<sub>crs</sub>*.

## **1.5 Thesis Overview**

The thesis is structured with six chapters starting with this introduction chapter explaining the basic CSP technologies. Chapter 2 discusses the literature study about various tubular receiver systems, receiver design methodology, design criteria and the heat transfer model.

Chapter 3 explains about the developed design methodology based on the study of various literatures. Chapter 4 describes the implementation of the developed design method which includes the structure of implementation and inputs/outputs of the developed model. Chapter 5 shows the results and validation of the developed design method. Finally, Chapter 6 concludes the work and discusses the possible future work.

# Chapter 2

## Literature Review

This chapter contains a brief literature survey about design methodology of tubular receivers implemented by several researchers. An overview of the design criteria and the existing heat transfer models of tubular receivers available in the literature are also discussed.

### 2.1 Tubular Receivers

Tubular receivers are the most widely used state of the art receiver technology [23]. There are four common system options available based on the receiver and storage fluid. The first two are state of the art systems and the other two are still in research phase.



Figure 2.1: Tubular receivers [43]

#### 2.1.1 Water/Steam

In this type of system, water is used as a heat transfer fluid (HTF) and so there is a direct steam generation in the receiver itself. One of the main advantages of this system is no need of heat exchanger if storage is not considered. But, the disadvantages of this system are

- Low receiver peak flux limit ( $0.3$  to  $0.6 \text{ MW/m}^2$ ) [18].
- Storing energy in the form of high-pressure steam is uneconomical and so the energy must be transferred to some other medium with heat exchangers resulting into higher energy loss.
- Two-phase heat transfer in the receiver directly influences its design.

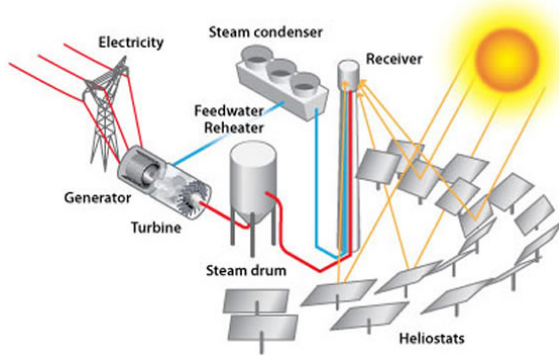


Figure 2.2: Flow layout of water/steam central receiver system [2]

- The pioneer CSP power plant, solar one used oil/rock thermocline storage. The maximum temperature limitation of oil is 315 °C and so the output steam from the storage has low temperature which results in the low turbine gross efficiency [18].

### 2.1.2 Molten Salt

Molten salt is an attractive HTF for CSP plants with storage because of its low cost and its commercial availability. Some of the attractive features [18] are

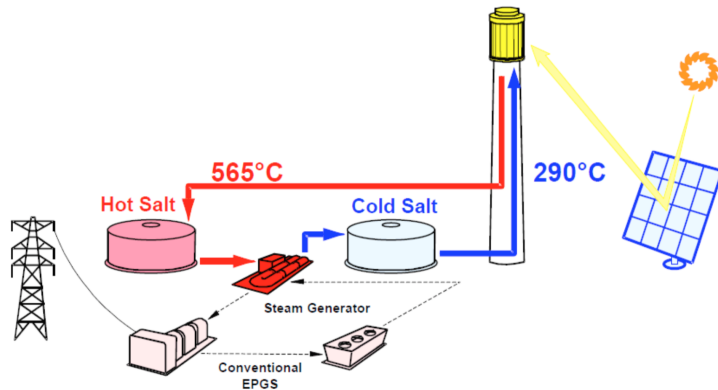


Figure 2.3: Flow layout of molten salt central receiver system [43]

- High receiver peak flux limit compared to water/steam system ( $0.6$  to  $0.8 \text{ MW/m}^2$ ).
- State of the art technology with 40 years of operational experience as an HTF.
- Non-toxic and stable over an extended period of time when protected from the environment and overheating.
- Molten salt is 2 to 3 times cheaper than sodium.

### 2.1.3 Liquid Sodium

Liquid sodium has very good heat transfer properties and so it has low thermal losses due to the reduced area of the receiver. Mostly, sodium receivers are external type with already reduced losses and so the further loss reduction with cavity type receiver is not shown to be beneficial [18]. Compared to molten salt, liquid sodium has very good heat transfer properties [18] which are given below:

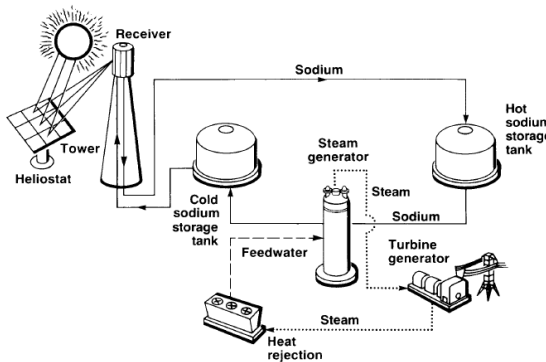


Figure 2.4: Flow layout of liquid sodium central receiver system [18]

- Receiver peak flux limit (in excess of  $1.5 \text{ MW/m}^2$ ).
- Higher thermal conductivity and so it is able to operate with high incident solar flux.
- Sodium has five times higher heat transfer rate than molten salt and so single pass is enough in the receiver fluid flow.
- Sodium freezes at  $100^\circ\text{C}$  which is two times lower when compared with molten salt.
- Sodium has higher boiling point ( $873^\circ\text{C}$ ) [10] which allows it to operate in other high-temperature cycles also.
- Because of the higher operational flux, receiver size, cost and its losses are reduced resulting into higher receiver efficiency. But, there are many limiting factors which act as a hindrance for sodium receiver to be commercially accomplished. Some of them [18] are stated below:
- The relatively high cost and low specific heat of sodium limit its usage as sensible heat storage medium.
- Low volumetric heat capacity of sodium makes the storage tank larger and costlier.
- The main point to note is that the highly reactive nature of sodium and water has to be considered while designing.

#### 2.1.4 Sodium/Salt Binary

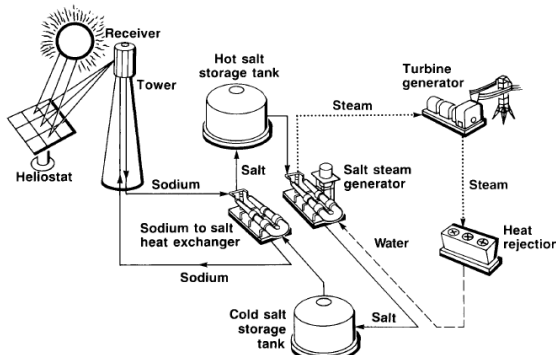


Figure 2.5: Flow layout of sodium/salt binary central receiver system [18]

The fourth option, in which sodium is used as a receiver fluid and molten salt is used as the storage fluid. It combines the attractive feature of both fluids but the additional heat transfer loop is needed to couple the system to run which adds complexity. The risk of sodium fire is reduced because it is restricted within the concrete tower but the reaction between sodium and molten salt is not well-known. Current indications are that it would be strongly exothermic and release the gaseous product which may cause pressurisation problem [18].

## **2.2 Receiver Design Methodology**

This section summarises the receiver design methodology suggested by various researchers.

### **2.2.1 Falcone [1986] [18]**

Falcone [18] suggested the following steps for the tubular receiver design:

1. Calculate the thermal rating of the receiver based on system level requirements like plant output, type of receiver fluid and storage media, nature of power cycle and solar multiple.
2. Select the flux limit based on working fluid and the tube material of the receiver.
3. Then, calculate the required receiver absorber area for the given allowable flux limit.
4. The receiver size should be within the limit of practical size.
5. The minimum receiver size is largely a function of spillage considerations based on the size of reflected heliostat beam and the size of its target. The beam size increases along with the size of heliostat even for the focused and canted mirrors. The receiver size also corresponds to reflected beam size in order to keep the spillage losses within a reasonable limit.
6. The maximum practical size is limited by the height of receiver panels due to shipping constraints.

### **2.2.2 Zavoico [2001] [45]**

Zavoico [45] suggested the following steps for the tubular receiver design:

1. Establish the allowable incident flux as a function of bulk salt temperature, allowable cumulative tube strains and corrosion rates at the salt film temperature.
2. Estimate the receiver size based on the maximum allowable flux.
3. Estimate the heat losses for various combinations of receiver height and diameter.
4. Then, the aspect ratio should be selected for the maximum receiver efficiency.
5. The dimensions of the receiver should be selected such that it gives the lower cost.

### **2.2.3 Lata [2008] [26]**

Lata [26] tried to optimize the receiver dimensions in order to increase the allowable peak flux of molten salt receiver from  $0.85 \text{ MW/m}^2$  to  $1 \text{ MW/m}^2$ . Basically, their design methodology is similar to other researchers. In addition, they tried to optimise the following receiver dimensions.

1. Receiver size optimisation to minimise the thermal losses (H/D ratio selection).
2. Small fluid cavity to maximise the receiver thermal efficiency and to prevent fatigue-creep damage (Tube diameter selection).
3. Thin walled conduction to improve thermal efficiency (Tube wall thickness selection).

4. Minimise the pressure losses by optimising the number of panels and molten salt circuit routeing (Number of panels and fluid path selection).
5. High nickel alloy material with excellent mechanical properties (Material selection).

All the above said design criteria for the receiver will be discussed in the next section.

#### 2.2.4 System Advisory Model (SAM) [43]

The performance model of SAM uses the TRNSYS components developed at the University of Wisconsin and the solar field optimisation algorithm is based on the DELSOL3 model developed at the Sandia national laboratory. It is capable of operating in two modes. The first one calculates the performance of an existing system. The second one is an optimisation of system design.

In the optimisation process, the tower height and receiver sizes are iteratively evaluated to find out the minimum possible cost of electricity output. But, the optimisation process needs the initial guess defined by the user. Then, the guess value is iteratively evaluated within the range given below. One of the limitation is that the educated guess of tower height has to be supplied by the user. It may mislead into wrong results if the guess value is not appropriate. The following are the ranges for the different parameters used for the optimisation.

- Nominal plant electric output power:  $\frac{1}{2}P_{el,guess} \leq P_{el,guess} \leq 5 \times P_{el,guess}$
- Tower height:  $0.6 \times H_{tower} \leq H_{tower} \leq 2 \times H_{tower}$
- Receiver Diameter:  $0.4 \times D_{rec} \leq D_{rec} \leq 1.8 \times D_{rec}$
- Height to Diameter ratio (Aspect ratio):  $0.6 \times \frac{H_{rec}}{D_{rec}} \leq \frac{H_{rec}}{D_{rec}} \leq 1.4 \times \frac{H_{rec}}{D_{rec}}$

They have developed objective function for the minimisation of the lowest energy cost and optimising iteratively based on the objective function by varying all the parameters within this range.

### 2.3 Design Criteria

The design criteria summarise about every parameter which needs to be optimised for better receiver design.

#### 2.3.1 Allowable Peak Flux Limit

The normal range of flux limit for the receiver fluids is tabulated below. It is based on the tube

Name of the HTF	Flux limit range	Unit
Water/Steam	0.3 to 0.6	$MW/m^2$
Molten Salt	0.6 to 0.85	$MW/m^2$
Liquid Sodium	1.2 to 1.3	$MW/m^2$

Table 2.1: Receiver flux limit for different HTF [18]

material and with the required number of life cycles. Figure 2.6 represents the graph of receiver peak flux for different HTF and materials [18]. In the graph, allowable flux limit of molten salt and sodium receiver with two types of steel are plotted with respect to life cycles. As a goal of 30

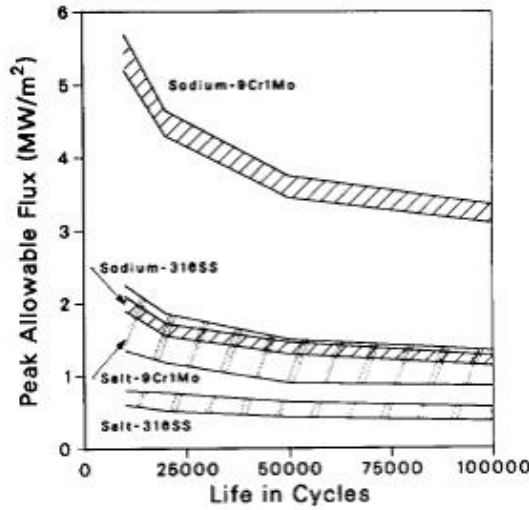


Figure 2.6: Receiver peak flux value for different HTF and materials with respect to life cycles [18]

years lifetime for the receiver, it would be roughly 11000 cycles at the rate of one cycle per day. But, one should take into account for the transients due to weather conditions also. The allowable peak flux,  $q_o$  can be calculated based on the simple model using the allowable thermal strain, thermal expansion and the poisson ratio of the material [28]. The average flux can be calculated by peak to average flux ratio. According to Stine and Harrigan [38], the peak to average flux ratio can be between 2 to 3.

$$q_o = \frac{\varepsilon}{\delta \left[ \frac{2}{1-v} R_{cond} + \frac{\pi}{\pi-1} \left( \frac{1}{2} R_{cond} + R_{conv} \right) \right]} \quad (2.1)$$

where

- $R_{cond} = \frac{d_o}{2k_m} \ln\left(\frac{d_o}{d_i}\right)$
- $R_{conv} = \frac{d_o}{d_i} h$
- $\varepsilon$  = Allowable strain of the material
- $\delta$  = Thermal expansion coefficient, 1/m K
- $v$  = Poisson's ratio
- $R$  = Thermal resistance, K/W
- $d$  = Diameter of the receiver tube, m
- $k$  = Thermal conductivity of the material, W/m K
- $h$  = Heat transfer coefficient, W/m² K

### 2.3.2 Receiver Sizing

Incident receiver thermal power should be estimated in order to size the receiver. Then, the allowable peak flux should be decided to calculate the absorber area required to handle the flux. The selection of the allowable peak flux has to be done carefully to avoid any failure. Generally, one-half to one-third of the peak flux [38] is selected as an average flux and the receiver is sized for the average flux in order to ensure that it would not fail.

For cavity receivers, the inner surfaces of the receiver are exposed to re-radiation because of the enclosed structure and it may lead to overheating. According to Falcone [18], the receiver size for cavity receivers is 25 percent larger than the external receiver for the same incident receiver thermal power. So, the average flux can be selected accordingly for the cavity receivers in order to ensure that it would not fail. Then, the receiver geometry is designed with the aim of lower cost and higher efficiency. The following section explains how to design the receiver geometry.

### 2.3.3 Receiver Aspect Ratio

According to the statement of Falcone [18], the receiver aspect ratio (height to diameter ratio) would be between 1 to 2. But, it should be optimised for minimum thermal losses and trade-off with spillage loss should also be considered. According to the statement of Zavoico [45], the receiver aspect ratio will be in the range of 1.2 to 1.5 but it should be selected for maximum receiver efficiency. For cavity receivers, it is known as height to width ratio which is usually in the range of 0.7 to 1 [18]. Some of the other design considerations from literatures [18] [45] are:

- The shipping constraint of the sub-assembly of panel tubes and the maximum continuous length of available seamless tubing limit the receiver height to 30m. But currently, there are some power plants which slightly crossed this limit. Crescent Dunes Solar Energy Project in US has the receiver height of 30.48 m [3] and the Atacama-1 project in Chile has been planned for the receiver height of 32 m [1].
- The larger height is desirable because of the high pointing accuracy of the heliostats (low spillage loss).
- The larger diameter is desirable to maximise the interior space available to place all the receiver components but resulting into increased thermal losses due to the larger diameter. So, space allocation design analysis should also be considered to optimise the aspect ratio.

### 2.3.4 Tube Diameter Selection

The receiver tube diameter can vary between 20 mm to 45 mm [26] and generally made of stainless steel or Incoloy. The analysis by Lata [26] states the following:

- Smaller the diameter, higher the receiver efficiency because it increases the salt velocity which in turn increases the heat transfer coefficient. But, the limitation of smaller diameter is that it increases the manufacturing cost and also the pressure drop due to the increased number of tubes.
- Pressure drop is directly proportional to the length of the salt circuit and to the square of the salt velocity and it is inversely proportional to the tube diameter. So, tradeoff between pressure drop and receiver efficiency should be done to optimise the tube diameter.
- Smaller the tube wall thickness, higher the heat transfer rates because it reduces the temperature gradients and therefore the efficiency is increased. But, the practical constraint is that the wall thickness is limited to commercial values.

### 2.3.5 Fluid Flow Path Selection

The fluid flow path is one of the main design considerations in order to avoid the uneven distribution of heat flux. Falcone [18] states that the upward fluid flow is preferable so that the buoyancy force of warmer does not counteract the pumping pressure. But for the molten salt receiver, multi-pass flow is needed and so it is difficult to design the upward fluid flow configuration in all the tubes. So, serpentine flow (up and down) is one of the best flow configurations. Wagner [43] developed a receiver model to analyse the behaviour of the solar power plants and he studied eight

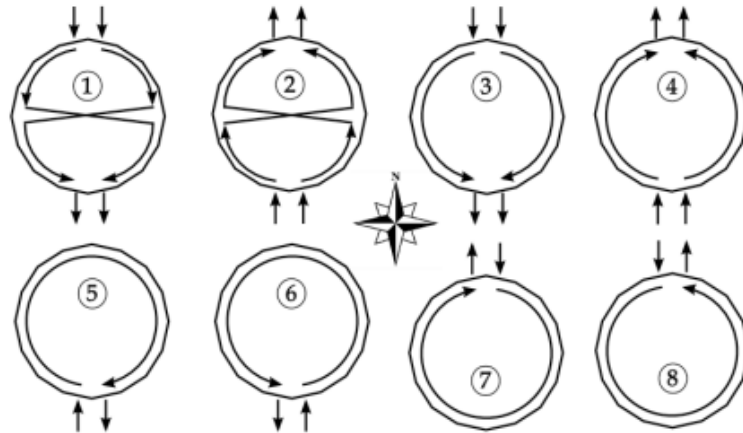


Figure 2.7: Eight possible fluid flow configuration by Wagner [43]

possible fluid flow configuration of the receiver. The following suggestions are given by Wagner [43] to design the efficient receiver:

- It is observed that the configuration with single flow path has higher pressure drop and so the parasitic pump power is increased. Hence, the two parallel flow path in the receiver is suggested in order to obtain the higher receiver thermal efficiency.
- In Northern hemisphere, the south to north flow configuration gives higher efficiency because if cold fluid enters the higher flux panel in northern side, it will lead to higher thermal losses.
- During peak flux, the hot fluid from the south side could not be able to cool the higher flux northern panel. So, the northern panels are exposed to higher thermal stresses during peak hours which is not recommendable.
- Hence, in the Northern hemisphere, the north to south flow configuration with two parallel flow path with or without a crossover is recommended for higher efficiency with low thermal stress.

Rodriguez-Sanchez [32] simulated the same eight flow configurations to select the best with the aim of increasing the receiver availability and the global efficiency of the solar tower plant. He also obtained the similar results like Wagner and he proposed that the north to south flow configuration with one crossover in the middle is the best configuration based on the considerations of receiver thermal efficiency, distributed flux, tube temperature and the thermal stress.

### 2.3.6 Tower Sizing

The tower height is mainly a function of the receiver thermal power of the plant [18]. The tower height is also influenced by the type of solar field. Falcone [18] presented the graph which shows the range of tower height for the given receiver thermal power and the type of solar field. The towers can be built of steel or concrete. Steel tower will look like wired microwave relay towers and the concrete tower will be similar to chimneys at industrial plants [18]. Figure 2.8 shows both steel and concrete type tower. The choice of selecting the type of tower mainly depends on the height of the tower [18]. The steel tower is shown to be beneficial below 120 m and concrete tower will be preferred for height more than 120 m [18]. The cost of tower increases with increasing tower height.

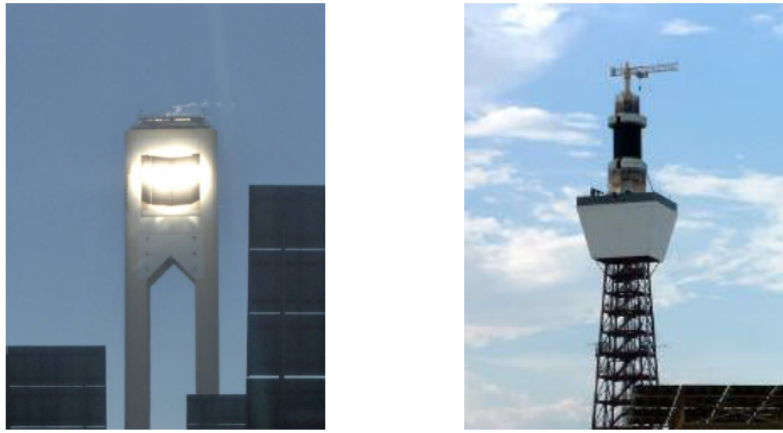


Figure 2.8: Solar tower for external and cavity receivers [19]

## 2.4 Cavity Specific Design Criteria

The following section consists of design criteria specific for cavity receivers. There is no specific design criteria needed for external receivers.

### 2.4.1 Cavity Receiver Geometry

The cavity receiver geometry is designed to reduce thermal losses by enclosing the absorber tubes inside the cavity. The receiver aspect ratio acts as a primary design parameter for the cavity receiver geometry which is generally 0.7 to 1 [18]. It decides the width and height of the aperture opening and the radius of the cavity. In the cavity receiver, all the piping and headers are placed inside the cavity and so there is some space needed on the top and bottom of the absorber tubes. It should be considered while designing the cavity receiver geometry. Generally, these spaces are covered by the lip to avoid heat losses. The design of lip is explained in the subsection lip height. Like active surfaces, the inactive surfaces are also heated up due to re-radiation and so careful selection of receiver allowable flux is necessary.

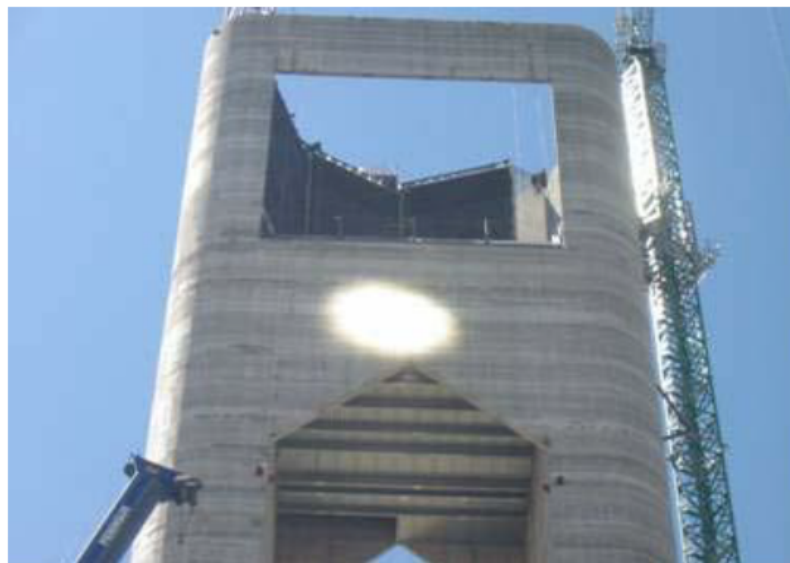


Figure 2.9: Cavity receiver with three of four receiver panels assembled in PS10 power plant [19]

### 2.4.2 Cavity Opening Angle

The cavity opening angle is the coverage angle of the radiation to the receiver from the solar field. Usually, the cavity opening angle is 180 degrees and the commercial plants like PS 10 are designed with the cavity opening angle of 180 degrees [19]. But, it actually depends on the solar field arrangement. Lukas [19] calculated the receiver thermal efficiency with the various cavity opening angle. He observed that the receiver thermal efficiency increases with the increasing cavity opening angle. It is explained that because of the decrease in aperture opening, heat loss will be lowered which in turn results in higher efficiency. But, it is not possible to distribute the heat flux uniformly for the higher cavity opening angle and so it can't be applied in real applications [19].

### 2.4.3 Lip Height (Aperture to Total Height Ratio)

The lip height which is usually specified as the aperture to total height ratio. The difference between the total height to aperture height is known as lip height. Generally, the upper lip reduces the heat losses and the lower lip does not have much effect on the heat losses [25]. The value of aperture to total height ratio used by Lukas is 0.75 [19]. If the aperture to total height ratio is further increased, it will decrease the heat loss but the spillage loss is increased. Hence, the tradeoff should be done in order to optimise the aperture to total height ratio.

### 2.4.4 Cavity Inclination

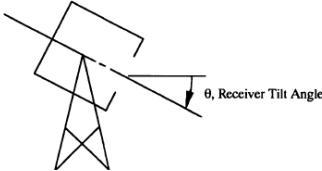


Figure 2.10: Cavity inclination angle [29]

The cavity inclination can vary from  $0^\circ$  to  $90^\circ$ . The convective heat loss of the cavity receiver depends on the wind speed, wind direction and also depends on the cavity inclination. Flesch [21] conducted the cryogenic wind tunnel experiment and observed the influence of wind on the convective loss for head on and side on wind direction. In the no wind condition, the convective heat loss decreases with increasing receiver tilt angle[15] [16]. But with higher wind speed, the higher tilt angle also contributes to higher losses. From the analysis of cryogenic wind tunnel experiment, Flesch [21] observed that the cavities should be designed in such a way that the wind flow is parallel to the aperture plane so that there is lesser wind influence to the heat losses. Moreover, cavity inclination is recommended in order to reduce the convection losses [21].

## 2.5 Heat Transfer Model

The heat loss model which consists of heat loss due to external convection, radiation and reflection. Conduction loss to the back side of the receiver panel is small compared to other losses [38] and so it is neglected in this study. The overview of various heat transfer models is summarised in this section. It is divided into two subsections as external and cavity receivers.

### 2.5.1 External Receiver

In the external receiver, the entire absorber area is exposed to the surroundings. So, there are higher thermal losses from the receiver to the surroundings when compared to cavity receivers.

The main thermal losses include convection and radiation heat loss.

### Convective Heat Loss

The heat transfer equations for the convection heat loss of cylindrical receivers are same like basic textbook equations. But, the Nusselt correlation that can be applied to the large-scale receivers is the ambiguous area in which a lot of researches are carried out [36] [12]. For the cylindrical receivers, heat transfer has an influence of both natural and the forced convection and so the mixed convection is usually considered [36]. In order to find out which heat transfer is dominant, Richardson number is used [40] and it is explained in the next subsection.

According to literatures [12] [36], heat transfer coefficient for mixed convection,  $h_{mix}$  can be stated with the following correlation. According to Cengel [12], the value  $m$  lies between 3 and 4. The value close to 3 suits better for vertical surfaces and the larger values are suited for horizontal surfaces. Siebers [36] studied this value particularly for both receivers and estimated the best-suited value of 3.2 and 1 for external and cavity receiver respectively.

$$h_{mix} = (h_{nat}^m + h_{for}^m)^{1/m} \quad (2.2)$$

where

- $h_{nat}$  = Heat transfer coefficient due to natural convection, W/m<sup>2</sup> K
- $h_{for}$  = Heat transfer coefficient due to forced convection, W/m<sup>2</sup> K

### Natural Convection Loss

The natural convection loss occurs due to buoyancy effects and the Nusselt correlation of the natural convection is given by many authors. The Nusselt correlation for the natural convection which can be applied for the large-scale solar external receiver is given below:

**Churchill and Chu [1975]:** This correlation is used for the design of base-load nitrate salt central power plant by Abengoa [41]. The research is carried out in Sandia national lab in US. All the fluid properties are calculated at the film temperature,  $T_f = \frac{T_{amb}+T_s}{2}$ .

$$Nu_{nat} = \left( 0.825 + \frac{0.387 Ra_L^{1/6}}{(1 + (0.492/\text{Pr})^{9/16})^{8/27}} \right)^2 \quad Ra_L < 10^{12} \quad (2.3)$$

For laminar flows, the following correlation is slightly more accurate. It is observed that a transition from laminar to turbulent boundary occurs when  $Re_L$  exceeds around  $10^9$ .

$$Nu_{nat} = \left( 0.68 + \frac{0.67 Ra_L^{1/4}}{(1 + (0.492/\text{Pr})^{9/16})^{4/9}} \right) \quad 10^{-1} < Ra_L < 10^9 \quad (2.4)$$

where

- Ra = Rayleigh number
- Pr = Prandtl number

Rayleigh number is defined as the product of Grashof number and the Prandtl number and it is given in the form of equation below:

$$Ra = Gr \cdot Pr \quad (2.5)$$

where

- Gr = Grashof number

The Grashof number can be calculated by the following equation:

$$Gr = g \cdot \beta \cdot (T_{s,ave} - T_{amb}) \cdot H_{rec}^3 / \nu_{fluid} \quad (2.6)$$

where

- $\beta$  = Volumetric expansion coefficient,  $1/K$
- $\nu_{fluid}$  = Kinematic viscosity,  $m^2/s$

Prandtl number is defined as the ratio of viscous diffusion rate and the thermal diffusion rate and it can be calculated by using the equation below:

$$Pr = \frac{\mu/\rho}{k/c_p\rho} = \frac{c_p\mu}{k} \quad (2.7)$$

where

- $\mu$  = Dynamic viscosity,  $kg/ms$

**Siebers and Kraabel [1984] [36]:** This correlation is widely used for the heat loss calculation of the solar receivers [14]. But, the author itself stated that there is nearly 40 percent uncertainty in the equation [36]. All the fluid properties are calculated at the ambient temperature.

$$Nu_{nat} = 0.098 \cdot Gr_H^{1/3} \cdot (T_s/T_{amb})^{-0.14} \quad (2.8)$$

### Forced Convection Loss

The forced convection loss occurs due to the influence of wind velocity and the Nusselt correlation for the forced convection which can be applied to the large-scale solar external receiver is described below:

**Churchill and Bernstein [1977] [12]:** The following correlation is valid for  $Re \cdot Pr > 0.2$  [12]. But, Christian and Clifford stated that this correlation is valid for Reynold's number up to  $4 \times 10^5$  and so this correlation can't be used for higher wind speeds [14]. All the fluid properties are calculated at the film temperature,  $T_f$ .

$$Nu_{for} = 0.3 + \frac{0.62 \cdot Re^{1/2} \cdot Pr^{1/3}}{[1 + (0.4/Pr)^{2/3}]^{1/4}} \left[ 1 + \left( \frac{Re}{282,000} \right)^{5/8} \right]^{4/5} \quad (2.9)$$

where

- $Re$  = Reynolds number

Reynolds number is defined as the ratio of inertial and the viscous forces and it can be calculated using the following equation:

$$Re = \frac{u_{wind} \cdot D_{rec}}{\nu_{air}} \quad (2.10)$$

where

- $u_{wind}$  = Wind velocity,  $m/s$

**Siebers and Kraabel [1984] [36]:** This correlation is widely used for the heat loss calculation of the solar receivers [14]. All the fluid properties are calculated at the film temperature,  $T_f$ . where

- $K_s/D_{rec}$  = Surface roughness
- $K_s$  = Radius of the receiver tube, m

	Reynolds Number Range	Correlation
$K_s/D_{rec} = 0$ (A smooth cylinder)		
(1)	All $Re$	$Nu_{for} = 0.3 + 0.488 \cdot Re^{0.5} \cdot \left(1 + \left(\frac{Re}{282000}\right)^{0.625}\right)^{0.8}$
$K_s/D_{rec} = 75 \times 10^{-5}$		
(2)	$Re \leq 7.0 \times 10^5$	Use correlation (1)
(3)	$7.0 \times 10^5 < Re < 2.2 \times 10^7$	$Nu_{for} = 2.57 \times 10^{-3} \cdot Re^{0.98}$
(4)	$Re \geq 2.2 \times 10^7$	$Nu_{for} = 0.0455 \cdot Re^{0.81}$
$K_s/D_{rec} = 300 \times 10^{-5}$		
(5)	$Re \leq 1.8 \times 10^5$	Use correlation (1)
(6)	$1.8 \times 10^5 < Re < 4 \times 10^6$	$Nu_{for} = 0.0135 \cdot Re^{0.89}$
(7)	$Re \geq 4 \times 10^6$	Use correlation (4)
$K_s/D_{rec} = 900 \times 10^{-5}$		
(8)	$Re \leq 1 \times 10^5$	Use correlation (1)
(9)	$Re > 1 \times 10^5$	Use correlation (4)

Table 2.2: Nusselt correlation for forced convection of external receivers [36]

**Cengel [2003] [12]:** In this correlation, the fluid can be either gas or liquid but it is valid between the Reynolds number range of  $4 \times 10^4 - 4 \times 10^5$ . This correlation is used for the design of base-load nitrate salt central power plant by Abengoa [41]. The research is carried out in Sandia national lab in US.

$$Nu_{for} = 0.027 \cdot Re^{0.805} \cdot Pr^{1/3} \quad (2.11)$$

### Radiative Heat Loss

The radiation heat loss,  $\dot{Q}_{loss,rad}$  is simple for external receivers and it can be calculated using Stefan-Boltzmann law. The external receiver is coated with the black coating to increase the absorptivity. Generally, black pyromark is used to coat the receiver panels and housing [45].

$$\dot{Q}_{loss,rad} = \sigma \cdot \epsilon_{rec} \cdot A_{rec} \cdot (T_{s,ave}^4 - T_{amb}^4) \quad (2.12)$$

where

- $\sigma$  = Stefan-Boltzmann constant,  $5.670 \cdot 10^{-8} W/m^2 K^4$
- $\epsilon_{rec}$  = Emissivity of the receiver
- $A_{rec}$  = Area of the receiver,  $m^2$
- $T_{s,ave}$  = Average surface temperature, K
- $T_{amb}$  = Ambient temperature, K.

### 2.5.2 Cavity Receiver

In this subsection, the heat transfer models specific for cavity receiver are discussed. In the cavity receivers, the absorber tubes are enclosed in a cavity to reduce the thermal losses. Like external receivers, the main thermal losses in the cavity receivers are convection heat loss and radiation heat loss.

#### Convective Heat Loss

Convection losses can be divided into natural convection due to buoyancy and forced convection due to the influence of wind velocity. In order to find out which heat transfer is predominant, the Richardson number can be used [40]. With the help of this number, it is easy to find out what kind of convection mechanism has to be included in the heat transfer model. Richardson number,  $Ri$  is defined as the ratio of Grashof number to the square of Reynolds number.

$$Ri = Gr/Re^2 \quad (2.13)$$

- If the Richardson number is greater than unity, natural convection dominates over the forced convection.
- If it is much lower than unity which indicates that natural convection is negligible and the forced convection dominates the heat transfer.

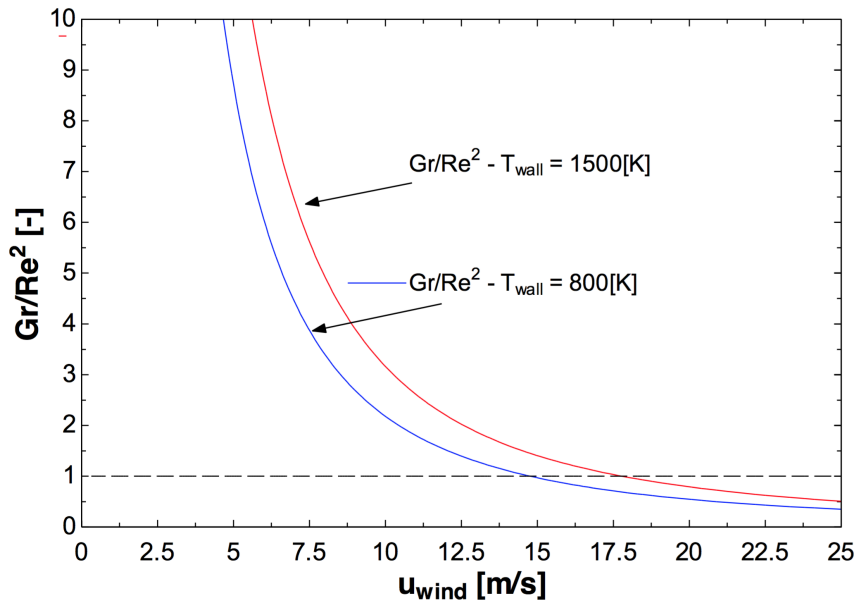


Figure 2.11: Variation of Richardson number with respect to wind velocity for cavity receiver [40]

In order to have an idea about Richardson number, Teichel [40] plotted the Richardson number with respect to varying wind speed shown in the Figure 2.11. From the Figure 2.11, one can conclude that the natural convection is dominant for the wind velocity less than 5 m/s. For wind velocities between 6 to 20 m/s, a mixed convection exists where both natural and forced convection have to be considered. For wind velocities higher than 25 m/s, the forced convection dominates and so the natural convection can be neglected.

Generally, the wind velocity can never exceed 20 m/s at the height of the receiver [40] and so only natural convection or mixed convection can be expected in the large central tower receivers. So, buoyancy effect has the significant influence on the heat transfer of convection losses.

However, the forced convection on large-scale cavity receivers has not been sufficiently studied. But, there are several studies on small scale cavity receivers [30] [39] and the heat losses due to wind velocity and direction [29] are also studied. Therefore, it is not well known whether these correlations can be applied to large central receivers of CSP towers.

### Natural Convection Loss

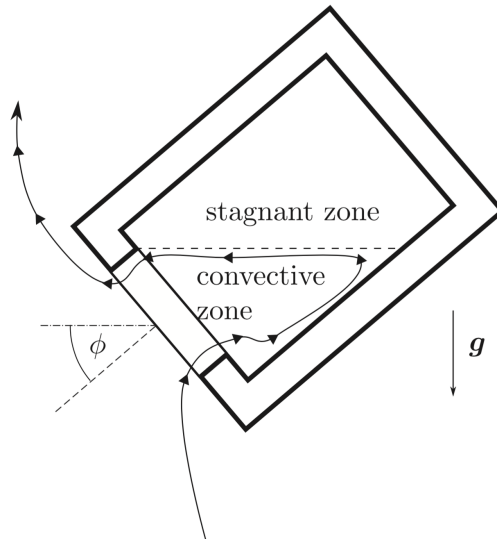


Figure 2.12: Two convection zones of the cavity receiver [21]

Convection heat loss for the cavity receiver can be well explained with the two-zone model. The figure shows the stagnant zone and convective zone of the cavity receiver.

- The stagnant zone is the region where the air is standing still and the temperature is close to the wall temperature [21].
- The convection zone is the region where the cold air enters through the aperture opening, gets heated up and leaves through the top of the aperture [21].

If the natural convection dominates, the stagnant zone is higher than the convective zone because the increasing wind speed can shrink the stagnant zone [21].

In 1983, Clausing [16] published the analytical and experimental modelling results with the test cavities in the cryogenic wind tunnel experiment conducted at the University of Illinois, Urbana-Champaign. Based on the results, he developed the natural convection heat transfer correlations and then he improved the correlations with the experimental work in 1987. Siebers and Kraabel [36] also came up with the natural convection heat transfer correlations in 1984 and it was based on the experimental work on cubical cavities by Kraabel.

**Clausing(1983) [16]:** According to Clausing, the circulating flow inside the cavity is mainly due to the buoyancy effects at boundary layers of the active surfaces [19]. However, it can be affected by the wind inflow and its direction. Clausing considered the wind velocity in the bulk flow velocity inside the cavity. Convection heat losses will not be greatly influenced by the wind velocity lower than 8 m/s. He developed the correlation which allows calculating the heat transfer coefficient specific for each surface separately.

This can be applied only if the heat transfer is dominated by internal resistance and the wind effect does not have high influence. This model is valid for Rayleigh number greater than  $1.6 \times 10^9$  and the temperature ratio of wall to ambient is between 1 and 2.6. It is numerically validated for the no-wind and the head-on wind conditions. According to Teichel [40], the temperature ratio of the receiver is between 1.8 and 3.4 and so it is out range for some conditions.

**Clausing(1987)** [17]: Clausing updated his previous model by experimental investigation of smooth, isothermal cubic cavity with a variety of side facing apertures to predict the convection loss for large-scale solar receivers. The large scale receivers are modelled using the cryogenic wind tunnel at the University of Illinois, Urbana Champaign. Using the results, Clausing came up with the correlation which was valid for larger Rayleigh numbers and the larger temperature ratio of wall to ambient so that it can be applied to large-scale solar receivers.

Unlike the previous model, this model is developed with only one heat transfer coefficient using the aperture area for the calculation of convection loss. This model is valid for  $3 \times 10^7 \leq Ra \leq 3 \times 10^{10}$  and  $1 \leq T_w/T_{amb} \leq 3$ . The actual receiver condition of large scale receivers can have still higher Rayleigh numbers and so it might not be valid for all cases [40].

**Siebers and Kraabel (1984)** [36]: Siebers and Kraabel developed the loss correlations for both cylindrical and cavity receivers which is based on the large and small scale experiments and also with the available literature. He considered natural convection in large cavities is similar to large vertical flat plates. He developed the Nusselt correlation for a simple cavity receiver with the validity range of  $10^5 \leq Gr \leq 10^{12}$ . Then, the heat transfer correlation is like the simple convection heat transfer. But, the correction factor is introduced in order to account for aperture lips and the tilt angle of the cavity. This model is validated with the experimental measurements and it shows good accordance with the results.

#### Forced Convection Loss

Forced convection has a significant influence on the convective heat transfer but there are no reliable correlations available to predict the forced convection heat transfer for the cavity receiver. The only simple correlation that can be applied to the cavity receiver is the correlation by Siebers and Kraabel [36]. They used the forced convection correlation for the vertical flat plate in order to account for the wind effect. It is also validated with the experimental data. The overall heat transfer coefficient can be obtained by adding the natural and forced convection heat transfer together.

While validating this correlation with 4.5 MW test receiver at Sandia Lab, the forced convection values are mostly over predicted and so it is a conservative model. The author states that the equation is expected to have an uncertainty of more than 50 percent [36].

#### Radiative Heat Loss

The radiation from active surfaces of the cavity receiver will directly or indirectly reach all the inactive surfaces and also it leaves to ambient through the aperture opening. It will re-radiate inside the cavity and will reach all active and inactive surfaces again. It is complex to find out the radiation heat losses accurately. But, it can be calculated by defining view factors and there are two widely used methods to calculate radiation heat loss [40]. They are

- Radiosity method
- F-hat method

But, the view factors can be calculated using analytical or by ray tracing method. The analytical method is limited to the specific cavity geometry and for other geometries, ray tracing is used.

# Chapter 3

## Design Methodology

This chapter consists of the design approach for tubular receivers and it also discusses the receiver design model for both external and cavity receivers.

### 3.1 Design Approach

1. The design method involves the calculation of the incident thermal power to the receiver as a first step. It can be calculated with the desired electric power output, power block efficiency, storage hours, solar multiple and the receiver thermal efficiency. In order to design the receiver, the efficiency is initially assumed to calculate the thermal power.
2. Once the thermal power is calculated, the type of receiver fluid and material needs to be selected.
3. Based on the type of heat transfer fluid and the receiver material, the allowable flux limit on the receiver can be chosen/calculated. After fixing the allowable flux limit, the receiver size can be calculated.
4. The next step is to design the receiver geometry in order to obtain maximum efficiency and the lower thermal stress in the receiver. The aspect ratio (height to diameter ratio) has to be chosen considering the factor of minimum thermal loss from the receiver. If the aspect ratio is fixed, then the height and diameter of the receiver will be known.
5. For the cavity receivers, the additional parameters like cavity opening angle, aperture to total height ratio and cavity inclination should be fixed to calculate the receiver geometry.
6. The tube diameter selection is one of the main design parameter, which needs to be selected in such a way that the pressure loss is minimised and the receiver efficiency is increased. Smaller diameter results in higher efficiency and the larger diameter tends to increase the pressure losses. Therefore, a trade-off between the receiver efficiency and the pressure loss should be considered in order to have a better overall efficiency.
7. The next step is selecting the tube thickness. Smaller thickness will lead to higher receiver efficiency, but it is limited by typical values of commercial tubes.
8. As a next step, the mass flow rate is calculated and the maximum design fluid flow velocity is fixed. Then, the cross-sectional area required for the fluid flow will be calculated using mass flow rate, velocity and the density of the fluid. Once the cross-sectional area is known, the number of tubes and panels can be calculated by selecting the number of flow path.
9. Now, the heat losses can be calculated for the designed receiver and the actual efficiency will be known. Hence, the receiver needs to be resized with actual efficiency and it is iterated until it converges.

10. Tower height sizing can be done with the receiver thermal power and the type of solar field.

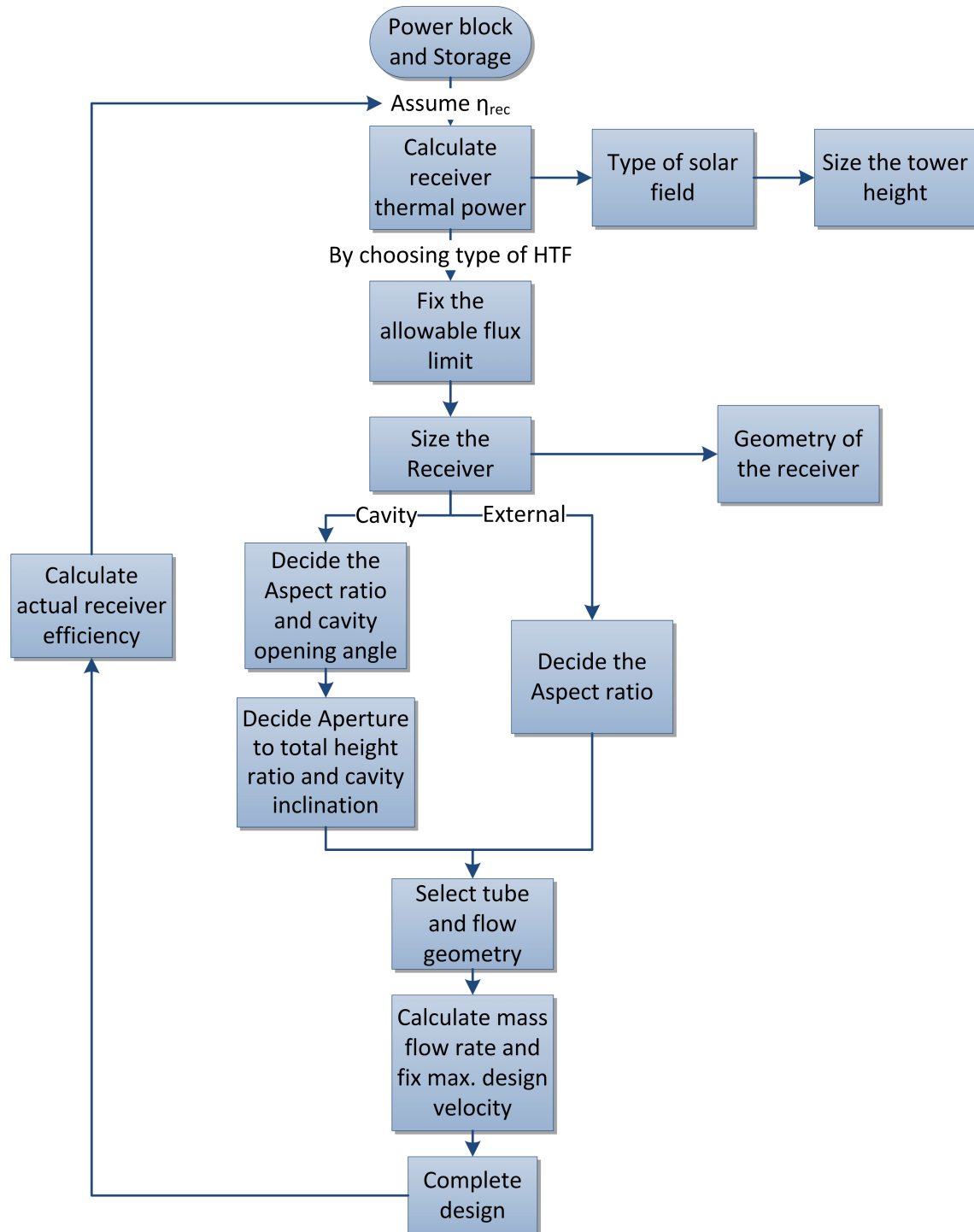


Figure 3.1: Receiver design methodology for tubular receivers

## 3.2 General Receiver Design Model

This section describes the receiver design model which is common for both external and cavity receivers.

### 3.2.1 Receiver Thermal Power

As it is explained in the design approach, the first step is to calculate the incident receiver thermal power. To calculate the receiver thermal power, thermal power required for the power block is obtained from the power block model, solar multiple is obtained from the solar multiple model and the receiver thermal efficiency is assumed. Then, the receiver thermal power,  $P_{th,rec}$  is calculated by

$$P_{th,rec} = \frac{P_{th,pb}}{\eta_{rec,guess}} \cdot SM \quad (3.1)$$

where

- $P_{th,pb}$  = Thermal power required for power block, W
- $\eta_{rec,guess}$  = Assumed receiver thermal efficiency
- $SM$  = Solar multiple

### 3.2.2 Calculation of HTF Properties

The properties of heat transfer fluid play a main role in the receiver design. The correlation of the properties is implemented for solar salt, hitec, hitec XL, therminol, liquid sodium and for some gases also [9]. In addition, there is a provision to specify the value of the HTF properties to simulate some other HTF as a receiver fluid. The properties needed for the receiver model are density, specific heat capacity, dynamic viscosity and the thermal conductivity. In this thesis, molten salt receiver is the main focus and the correlation used to calculate the molten salt (solar salt) properties are given in the Table 3.1.

Property	Equation	Units
Density	$\rho = 2090 - (0.636 \cdot T_{mean,htf})$	$kg/m^3$
Specific heat capacity	$C_p = 1443 + 0.172 \cdot T_{mean,htf}$	$J/kgK$
Dynamic viscosity	$\mu = (22.714 - (0.120 \cdot T_{mean,htf}) + (2.281 \times 10^{-4} \cdot T_{mean,htf}^2) - (1.474 \times 10^{-7} \cdot T_{mean,htf}^3))/10^3$	Pa s
Thermal conductivity	$k = 0.443 + 1.9 \cdot 10^{-4} \cdot T_{mean,htf}$	$W/m K$

Table 3.1: Properties of solar salt [45]

where

- $T_{mean,htf}$  is the mean fluid temperature in degree Celsius, °C

### 3.2.3 Receiver Sizing

Receiver sizing is done based on the allowable flux on the receiver. The allowable flux on the receiver depends on the receiver material and the type of the heat transfer fluid. Generally, the allowable peak flux for molten salt receiver fluid with 316 Stainless steel material is  $0.83 \text{ MW}/m^2$  [18] and with Incoloy 800H is  $1 \text{ MW}/m^2$  [28] [45]. So, these values are used as default values in the model. The average allowable flux can be calculated by the peak to average flux ratio. Falcone used a specific value of 1.78 for external receivers and 2.65 for cavity receivers [18]. Because of

re-radiation, cavity receivers have the higher peak to average flux ratio and so the receiver size is larger for the same receiver thermal power. The value used by Falcone is also in accordance with the Gemasolar design flux and hence it is used in this model. Using the average allowable flux, the area of the receiver,  $A_{rec}$  can be calculated by

$$A_{rec} = \frac{\dot{Q}_{th,rec}}{Q_{ave,flux}} \quad (3.2)$$

where

- $Q_{ave,flux}$  = Allowable average flux of the receiver,  $W/m^2$
- $\dot{Q}_{th,rec}$  = Incident receiver thermal power,  $W$

### 3.2.4 Receiver Surface Temperature Calculation

It is assumed that the receiver has a uniform surface temperature. The heat transfer through the tube walls is calculated and it includes conduction through the tube wall thickness and then convection to the receiver fluid. The surface temperature of the receiver is calculated by calculating resistance due to conduction and convection. The thermal power in the receiver fluid,  $\dot{Q}_{fluid}$  can be obtained by:

$$\dot{Q}_{fluid} = \frac{T_{s,ave} - T_{htf,ave}}{R_{cond} + R_{conv}} \quad (3.3)$$

where

- $T_{s,ave}$  = Average surface temperature of the receiver,  $K$
- $T_{htf,ave}$  = Average temperature of the receiver fluid,  $K$
- $R_{cond}$  = Resistance due to conduction through tube walls,  $K/W$
- $R_{conv}$  = Resistance due to internal convection between tube wall and the receiver fluid,  $K/W$

$$R_{cond} = \frac{\ln(r_{o,tube}/r_{i,tube})}{2 \cdot \pi \cdot H_{rec} \cdot k_{tube} \cdot n_{tube}} \quad (3.4)$$

where

- $r_{o,tube}$  = Radius of the receiver outer tube,  $m$
- $r_{i,tube}$  = Radius of the receiver inner tube,  $m$
- $k_{tube}$  = Thermal conductivity of the receiver tube,  $W/mK$
- $n_{tube}$  = Total number of tubes in the receiver
- $H_{rec}$  = Height of the receiver,  $m$

$$R_{conv} = \frac{1}{h_{inner} \cdot \pi \cdot r_{i,tube} \cdot H_{rec} \cdot n_{tube}} \quad (3.5)$$

where

- $h_{inner}$  = Heat transfer coefficient of internal convection between tube wall and the receiver fluid,  $W/m^2K$

$$h_{inner} = Nu \cdot k_{fluid}/L_c \quad (3.6)$$

where

- $Nu$  = Nusselt number

- $L_c$  = Characteristic length

The Nusselt correlation,  $Nu$  by Dittus-Boelter [9] is used and it is given by,

$$Nu = 0.023Re^{0.8}Pr^{0.4} \quad (3.7)$$

where

- $Re$  = Reynolds number
- $Pr$  = Prandtl number

The above equation is valid for  $0.7 < Pr < 120$  and  $10^4 < Re < 1.2 \times 10^5$ . Using these equations, the surface temperature of the receiver is calculated.

### 3.2.5 Mass Flow Rate Calculation

The design mass flow rate of the receiver fluid is calculated with the incident receiver thermal power and the thermal efficiency of the receiver. The minimum limitation of the mass flow rate to avoid any damage is to make sure that the flow is turbulent. So, it can be calculated with the Reynolds number greater than or equal to 4000 [32]. The mass flow rate,  $\dot{m}_{htf}$  is calculated by

$$\dot{m}_{htf} = \frac{\dot{Q}_{inc,rec} \cdot \eta_{rec}}{cp_{htf,ave} \cdot (T_{htf,hot} - T_{htf,cold})} \quad (3.8)$$

where

- $\eta_{rec}$  = Receiver thermal efficiency
- $cp_{htf,ave}$  = Specific heat of the receiver fluid, J/kg K
- $T_{htf,hot}$  = Outlet temperature of the hot receiver fluid, K
- $T_{htf,cold}$  = Inlet temperature of the cold receiver fluid, K

### 3.2.6 Pressure Loss and Pump Power Calculation

The pressure drop across the receiver tube is given by the following equation. The pressure loss due to the bends is not considered in this model. The pressure loss model is very simple model to estimate the approximate pressure loss in the receiver tubes.

$$\Delta P_{tube} = \rho_{fluid} \cdot f \cdot \frac{H_{rec}}{D_{tube,inner}} \cdot \frac{v_{fluid}^2}{2} \quad (3.9)$$

where  $f = (0.790 \ln Re - 1.64)^{-2}$  for smooth tubes valid for  $10^4 < Re < 10^6$  and for rough tubes  $f = \frac{1}{\sqrt{f}} = -2.0 \log \left( \frac{\epsilon/D}{3.7} + \frac{2.51}{Re\sqrt{f}} \right)$

where

- $\Delta P_{tube}$  = Pressure loss through the receiver tube, Pa
- $\rho_{fluid}$  = Density of the receiver fluid, kg/m<sup>3</sup>
- $v_{fluid}$  = Velocity of the receiver fluid, m/s
- $\epsilon/D$  = Relative roughness

The pressure drop for pumping the fluid up to the receiver is given by

$$\Delta P_{tower} = \rho_{fluid} \cdot g \cdot H_{tower} \quad (3.10)$$

where

- $\Delta P_{tower}$  = Pressure loss through the pumping of receiver fluid upto the tower, Pa
- $H_{tower}$  = Height of the tower, m

The net pressure drop across the receiver panels are given by

$$\Delta P_{net} = (\Delta P_{tube} \cdot n_{panels}/n_{flowpath}) + \Delta P_{tower} \quad (3.11)$$

where

- $\Delta P_{net}$  = Net pressure loss through the receiver panels, Pa
- $n_{panels}$  = Number of panels in the receiver
- $n_{flowpath}$  = Number of flow path in the receiver

The energy required to pump the receiver fluid through the receiver is given by

$$\dot{W}_{pump} = \frac{\Delta P_{net} \cdot v_{fluid} \cdot \frac{\pi D_{tube,inner}^2}{4} \cdot n_{tubes,panel}}{\eta_{pump}} \quad (3.12)$$

where

- $\dot{W}_{pump}$  = Parasitic pump power required for the receiver, W
- $n_{tubes,panel}$  = Number of tubes per panel in the receiver
- $\eta_{pump}$  = Pump efficiency

### 3.3 External Receiver Design Model

#### 3.3.1 Geometry Design

For the external receiver, the outer geometry design includes diameter and height of the receiver. In order to design the outer geometry, the parameter receiver aspect ratio (Height to diameter ratio) should be introduced. Usually for an external receiver, the aspect ratio lies between 1 to 2 [18]. In this model, the default value of receiver aspect ratio is set as 1.5. The area of the receiver can be written as

$$A_{rec} = \pi \cdot D_{rec} \cdot H_{rec} \cdot \pi/2 \quad (3.13)$$

The curvature of the tubes is also included in the receiver absorber area and so the allowable average flux can also be calculated for the same. The above equation can be reformulated in terms of receiver aspect ratio and the geometry can be calculated as

$$D_{rec} = \sqrt{A_{rec}/(\pi \cdot h/d_{ratio} \cdot \pi/2)} \quad (3.14)$$

$$H_{rec} = h/d_{ratio} \cdot D_{rec} \quad (3.15)$$

where

- $D_{rec}$  = Diameter of the receiver, m
- $h/d_{ratio}$  = Receiver aspect ratio
- $\pi/2$  = Factor due to the curvature of the receiver tubes

### 3.3.2 Tube and Panel Design

In order to design receiver tube and panel, the tube outer diameter, the tube thickness and the number of flow path in the receiver should be selected. The tube outer diameter usually varies between 20 mm to 45 mm [26]. It will vary based on the receiver thermal power. Because of the fact that mass flow rate of the fluid will be varied to meet the required receiver thermal power. Consequently, the fluid velocity will be varied to meet the required mass flow. So, the cross-sectional area should be adjusted to maintain the fluid velocity within the allowable limit.

Scalability of the power plant is addressed by developing the linear correlation for tube outer diameter with receiver thermal power. The linear correlation will act as a default value when the user does not specify any value of tube outer diameter. It is developed with the two extreme cases of a commercial power plant. The 10 MW power plant with 2 hours of storage and the 100 MW power plant with 14 hours of thermal storage are considered as the two extremes. The tube outer diameter is 12.7 mm [37] and 40.9 mm [41] respectively. The developed linear correlation for tube outer diameter,  $d_{o,tube}$  is shown below:

$$d_{o,tube} = (0.00004827128 \cdot P_{th,rec}/1000000) + 0.01062434 \quad (3.16)$$

Tube thickness depends on the pressure exerted by the fluid onto the tube. For instance, direct water/steam receiver needs thicker tubes to hold the higher pressure. It can be as low as 1 mm for the molten salt receiver. As a conservative approach, the default value of tube thickness is selected as 2 mm in this model.

Wagner [43] suggested the number of flow path as 2 for the efficient receiver and so the default value is selected as 2 in this model. The total number of receiver tubes,  $n_{tube,rec}$  can be calculated as

$$n_{tube,rec} = \frac{\pi \cdot D_{rec}}{d_{o,tube}} \quad (3.17)$$

Then, the number of panels in the receiver,  $n_{panels}$  can be calculated by calculating the number of tubes per panel,  $n_{tube,panel}$ . It can be calculated by knowing the cross sectional area of the fluid which are given below:

$$n_{tube,panel} = \frac{A_{sec}}{\pi \cdot (d_{i,tube}/2)^2 \cdot n_{flowpath}} \quad (3.18)$$

where

- $A_{sec}$  = Cross sectional area of the fluid flow path

$$A_{sec} = \frac{\dot{m}_{htf}}{\rho_{fluid} \cdot v_{fluid}} \quad (3.19)$$

Once the number of tubes per panel is calculated, the number of receiver panels,  $n_{panels}$  can be calculated as

$$n_{panels} = \frac{n_{tube,rec}}{n_{tube,panel}} \quad (3.20)$$

While designing, it should be taken care that the number of panels will also be even if the number of flow path is even. In this model, a condition is written to check and adjust the number of panels to the very next even number.

### 3.3.3 Tower Height Design

Currently, there is no reliable tower height model in the literature. Tower height is given as a user input in all the commercial design software. In this model, either user can give input for tower height or the default values are selected within the tool chain. Falcone [18] has given the graph for tower height with respect to the receiver thermal power and so the correlation is developed by

curve fitting with his values. It can act as default values for tower height in the developed receiver model. The graph by Falcone is shown in Figure 3.2. The correlation for calculating tower height for surround field is given below:

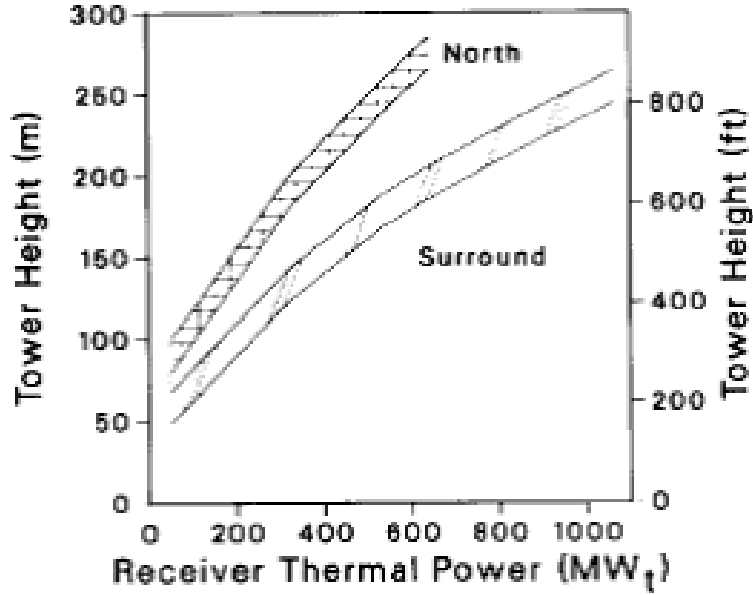


Figure 3.2: Variation of tower height with respect to receiver thermal power [18]

$$H_{tower,min} = 36.30075 + (0.3013896 \cdot P_{th,rec}) - (0.0001004369 \cdot P_{th,rec}^2) \quad (3.21)$$

$$H_{tower,max} = 54.91579 + (0.3070526 \cdot P_{th,rec}) - (0.0001039793 \cdot P_{th,rec}^2) \quad (3.22)$$

$$H_{tower} = \frac{H_{tower,min} + H_{tower,max}}{2} \quad (3.23)$$

where

- $H_{tower,min}$  = Minimum tower height, m
- $H_{tower,max}$  = Maximum tower height, m
- $H_{tower}$  = Tower height, m

### 3.3.4 Receiver Thermal Efficiency

The receiver thermal efficiency is calculated by defining all thermal losses from the receiver.

$$\eta_{rec} = 1 - \frac{Q_{loss,tot}}{P_{th,rec}} \quad (3.24)$$

where

- $\eta_{rec}$  = Receiver thermal efficiency
- $Q_{loss,tot}$  = Total heat loss from the receiver, W

The heat loss model includes heat loss due to reflection, external convection and radiation. The conduction to the back side of the receiver panel is small compared to other losses and it is neglected [38].

$$\dot{Q}_{loss,tot} = \dot{Q}_{loss,ref} + \dot{Q}_{loss,conv} + \dot{Q}_{loss,rad} \quad (3.25)$$

where

- $\dot{Q}_{loss,ref}$  = Heat loss due to reflection,  $W$
- $\dot{Q}_{loss,conv}$  = Heat loss due to external convection,  $W$
- $\dot{Q}_{loss,rad}$  = Heat loss due to radiation,  $W$

### Reflection Heat Loss

The part of the radiation which are reflected away from the receiver surface is called reflective heat loss. It can be calculated by using the absorptance of the receiver coating. The following equation gives the reflective heat loss from the receiver surface:

$$\dot{Q}_{loss,ref} = (1 - \alpha_{eff}) \cdot P_{th,rec} \quad (3.26)$$

where

- $\alpha_{eff}$  = Effective absorptance due to the curvature of receiver tubes
- $\alpha$  = Absorptance of the paint

The curvature of the tubes has to be taken into account while calculating absorptance. The effective absorptance can be calculated by:

$$\alpha_{eff} = \frac{\alpha}{\alpha + (1 - \alpha) \frac{A_{abs}}{A_{env}}} \quad (3.27)$$

where

- $A_{abs}$  = Area of the absorber,  $m^2$
- $A_{env}$  = Projected area of the envelope without considering the curvature of tubes,  $m^2$

### Convection Heat Loss

The external receiver is usually approximated as a cylinder. It is considered as a vertical cylinder for the heat transfer model. The height of the receiver is always higher than the diameter and it agrees to the following condition to treat the receiver as vertical plate for the heat transfer correlations.

$$\frac{D_{rec}}{H_{rec}} \geq \frac{35}{Gr_L^{\frac{1}{4}}} \quad (3.28)$$

The external convection heat loss equation is given below with the mixed convection heat transfer coefficient.

$$\dot{Q}_{loss,conv} = h_{mix} \cdot A_{rec} \cdot (T_{s,ave} - T_{amb}) \quad (3.29)$$

where

- $h_{mix}$  = Heat transfer coefficient due to mixed convection,  $W/m^2K$

**Mixed convection:**

According to literatures [36], most of the external solar receivers will undergo mixed convection. So, mixed convection is used in this model. It can be stated with the correlation [12] [36] which is given in equation 2.2.

**Natural convection:**

The heat transfer coefficient for natural convection,  $h_{nat}$  can be calculated with the following equation:

$$h_{nat} = Nu_{nat} \cdot k_{air}/L_c \quad (3.30)$$

In this thesis, Siebers and Kraabel correlation is used for the heat transfer model because of its wide validity range and it is developed especially for large-scale solar receivers based on the experiments. Siebers and Kraabel correlation is given in the equation 2.8.

**Forced convection:**

The heat transfer coefficient for forced convection,  $h_{for}$  can be calculated with the following equation:

$$h_{for} = Nu_{for} \cdot k_{air}/D_{rec} \quad (3.31)$$

Like natural convection, Siebers and Kraabel correlation is used for the forced convection also due to its wide validity range and it is developed for large-scale solar receivers. In the Table 2.2, Nusselt correlation for smooth and rough cylinders are shown.

**Radiative Heat Transfer**

The radiative heat transfer for external convection is very simple and the Stefan-Boltzmann equation is used to calculate the radiative heat loss. It is explained in the section 2.

## 3.4 Cavity Receiver Design Model

### 3.4.1 Geometry Design

Geometry design includes the radius of the cavity, height of the receiver, height of the absorber, lip height, width and height of the aperture, cavity opening angle and the cavity inclination angle. Aspect ratio should be decided to design cavity receivers. It usually ranges between 0.7 to 1 for cavity receivers [18]. Receiver aspect ratio is shown in the Figure 3.3 where  $H_P/W_A$  is the height to width ratio or receiver aspect ratio.

The following steps show how to calculate the width and height of the receiver aperture. Once the absorber area is calculated with the allowable heat flux, width and height of the receiver aperture can be calculated by fixing aspect ratio and the cavity opening angle.

$$A_{abs} = \frac{\theta_{rec}}{180} \cdot \pi \cdot R_{rec} \cdot H_{abs} \cdot \frac{\pi}{2} \quad (3.32)$$

where

- $A_{abs}$  = Receiver absorber area,  $m^2$
- $\theta_{rec}$  = Cavity opening angle in degrees,  $^\circ$
- $R_{rec}$  = Radius of the receiver,  $m$
- $H_{abs}$  = Height of the absorber,  $m$

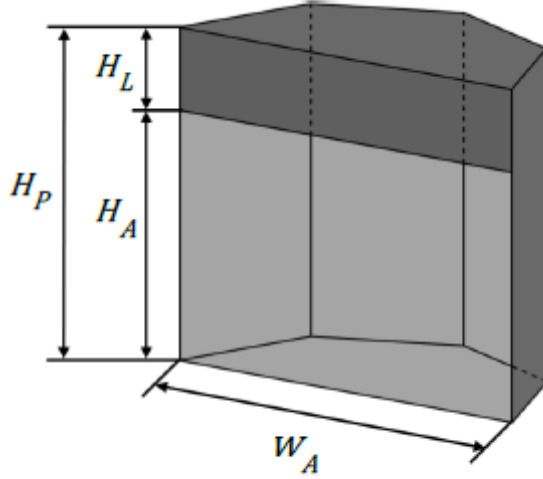


Figure 3.3: Geometry of cavity receiver [19]

The radius and height of the absorber can be calculated by rewriting the above equation in terms of aspect ratio which is shown below. In order to have an idea of receiver radius and its internal angle geometry, it is shown in the Figure 3.4. The aperture width,  $W_{aper}$  can be calculated from the following equation with the assumption of receiver width always equals to aperture width or by fixing aperture to total width ratio:

$$W_{aper} = 2R_{rec} \cos\left(\frac{\pi - \theta_{rec}}{2}\right) \quad (3.33)$$

$$H_{aper} = h/d_{ratio} \cdot 2 \cdot R_{rec} \quad (3.34)$$

where

- $H_{aper}$  = Aperture height of the receiver, m

$$R_{rec} = \sqrt{\frac{A_{abs}}{\frac{\theta_{rec}}{\pi} \cdot \pi^2 \cdot h/d_{ratio}}} \quad (3.35)$$

In order to accommodate the receiver pipings and headers inside the cavity, extra space should be needed. After including the space, the overall height can be calculated with the parameter

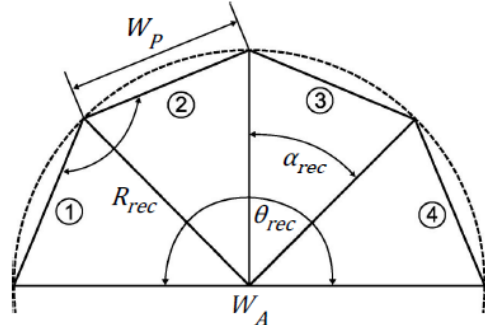


Figure 3.4: Internal angle geometry of cavity receiver [19]

aperture to total height ratio. The extra spacing is covered by the lip in the cavity. Only upper lip is considered in the current model. The aperture to total height of the receiver is chosen as 0.75 and the total height and lip height of the receiver can be calculated by

$$H_{rec} = \frac{1}{\left(\frac{h_{aper}}{h_{tot}}\right)_{ratio}} \cdot H_{abs} \quad (3.36)$$

$$H_{lip} = H_{rec} - H_{abs} \quad (3.37)$$

where

- $H_{lip}$  = Lip height of the receiver,  $m$
- $\left(\frac{h_{aper}}{h_{tot}}\right)_{ratio}$  = Aperture to total height ratio

### 3.4.2 Tube and Panel Design

The receiver tube and panel design is more same like external receivers except the calculation of number of receiver tubes in the receiver. The number of receiver tubes can be calculated by

$$n_{tube,rec} = \frac{\pi \cdot R_{rec} \cdot \frac{\theta_{rec}}{\pi}}{d_{tube,outter}} \quad (3.38)$$

### 3.4.3 Tower Height Design

The tower height for cavity receiver is calculated by the correlation developed by curve fitting Falcone values. The correlation is shown below:

$$H_{tower,min} = 58.31818 + (0.4377023 \cdot P_{th,rec}) - (0.0001802198 \cdot P_{th,rec}^2) \quad (3.39)$$

$$H_{tower,max} = 76.02273 + (0.4571479 \cdot P_{th,rec}) - (0.0002080919 \cdot P_{th,rec}^2) \quad (3.40)$$

$$H_{tower} = (H_{tower,min} + H_{tower,max})/2 \quad (3.41)$$

### 3.4.4 Receiver Thermal Efficiency

The general procedure for calculation of receiver thermal efficiency is same as that of external receivers. The heat losses which are different for cavity receivers are shown below.

#### Reflection Heat Loss

The reflection heat loss is reduced because of the enclosed cavity and the reflected radiation can only pass through the aperture to reach the ambient. The simple reflection loss equation is derived by assuming the receiver thermal power is uniformly distributed throughout the receiver. The following equation is used to calculate the reflected heat loss from the cavity receiver:

$$\dot{Q}_{loss,ref} = (1 - \alpha_{eff}) \cdot \frac{P_{th,rec}}{A_{abs}} \cdot A_{aper} \quad (3.42)$$

where

- $A_{aper}$  = Area of the aperture,  $m^2$

### Convection Heat Loss

In the cavity receiver, the convection heat loss can be reduced because the absorber tubes are not directly exposed to the surroundings. Also, the direct wind influence is protected by the cavity structure and the heated air inside the cavity is also blocked by the closed ceiling. Therefore, it is assumed that the inactive surfaces and the air inside the cavity are in the higher temperatures due to re-radiation.

#### Natural convection:

The following Nusselt correlation by Siebers can be used to calculate the natural heat transfer

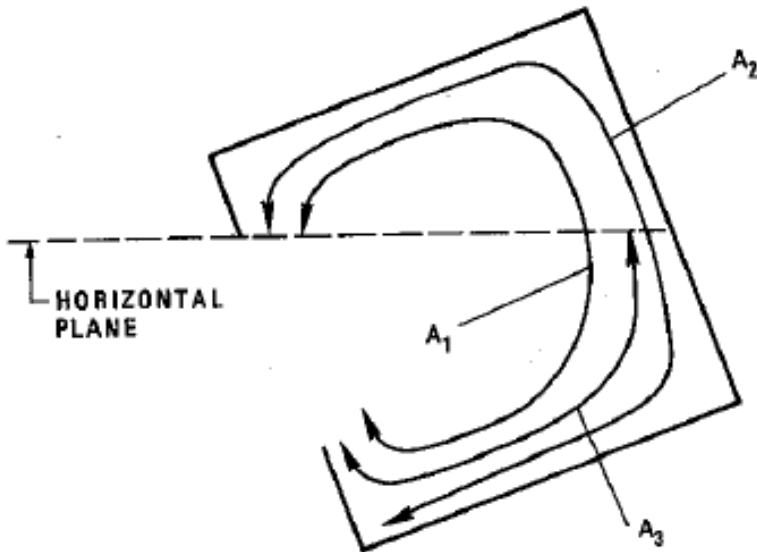


Figure 3.5: Internal heat transfer area of the cavity receiver [36]

coefficient:

$$Nu_l = 0.088Gr_l^{1/3} \left( \frac{T_w}{T_{amb}} \right)^{0.18} \quad 10^5 \leq Gr \leq 10^{12} \quad (3.43)$$

The direct heat transfer coefficient correlation for air at normal atmospheric temperatures is given by:

$$h_{nc,0} = 0.81(T_w - T_{amb})^{0.426} \quad (3.44)$$

$$h_{nc} = h_{nc,0} \left( \frac{A_1}{A_2} \right) \left( \frac{A_3}{A_1} \right)^n \quad (3.45)$$

where

- n is 0.63 and for cavities inclined more than  $30^\circ$ , n is 0.8
- Area  $A_1$ ,  $A_2$  and  $A_3$  are shown in the Figure 3.5.

The area used for heat transfer is the total interior surface of the cavity receiver,  $A_1$ .

#### Forced convection:

The following Nusselt correlations by Siebers can be used to calculate the forced heat transfer coefficient:

$$Nu_W = 0.0287Re_W^{0.8}Pr^{1/3} \quad (3.46)$$

The area used for heat transfer is the aperture area of the cavity receiver.

### Radiation Heat Loss

In this thesis, the simple radiation loss model is derived with aperture opening area by assuming the uniform temperature inside the cavity and by using enclosure and reciprocity rule. The cavity receiver is coated with the black coating to increase the absorptivity. Generally, black pyromark is used to coat the receiver panels and housing [45]. The following equation is used to calculate the radiation heat loss from the cavity receiver:

$$\dot{Q}_{loss,rad} = \sigma_S \cdot \epsilon_{rec} \cdot A_{aper} \cdot (T_{s,ave}^4 - T_{amb}^4) \quad (3.47)$$

where

- $\sigma_S = 5.670 \cdot 10^{-8} W/m^2 K^4$  is Stefan-Boltzmann constant,
- $\epsilon_{rec} = 0.83$  the emissivity of black pyromark [45].

This is valid if the average surface temperature of all surfaces inside the cavity is used.

# Chapter 4

## Implementation of the Design Method

The main aim of this thesis focuses on the implementation of design method for external and cavity receivers in the in-house solar tower power plant design tool  $devISE_{crs}$ . This section describes the general overview of the Fraunhofer in-house solar power tower software and the implementation structure of the receiver module in the tool.

### 4.1 Software Description

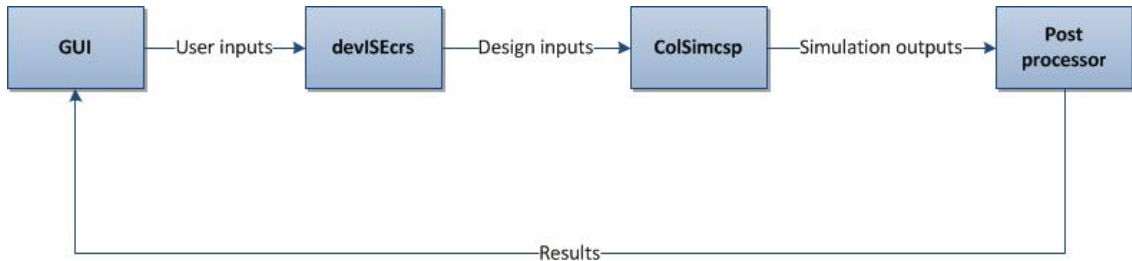


Figure 4.1: General structure of the in-house solar tower power plant design and simulation software

As seen in the Figure 4.1,  $devISE_{crs}$  is embedded in the ISE in-house tool for the design and simulation of the solar tower power plant. The brief function of each tool includes:

- GUI (Graphical User Interface): It is used to get the inputs parameters from the users.
- $devISE_{crs}$ : A design tool to size the power plant based on the specified input parameters and to design all the sub modules of the power plant.
- $ColSim_{csp}$ : A transient plant simulation software which assess the annual yield of the power plant.
- Post processor: A post processor which return the results back to the GUI for displaying to the user.

The role of the  $devISE_{crs}$  is the design part and to supply the inputs needed for the  $ColSim_{csp}$ . The following section describes about the  $devISE_{crs}$  tool and its several modules.

## 4.2 *devISE<sub>crs</sub>* - A Design Tool

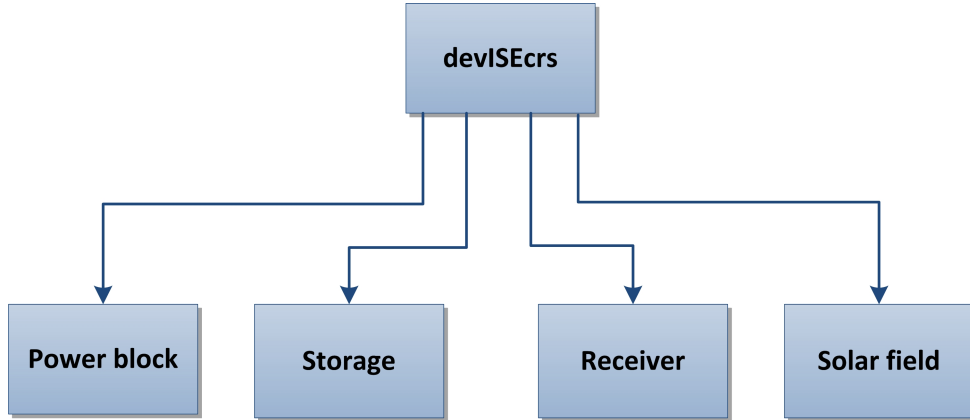


Figure 4.2: Modules of the *devISE<sub>crs</sub>* design tool

There are four main modules in the *devISE<sub>crs</sub>* tool which will be discussed below:

- The power block is the first module in the design tool and it computes the thermal power required for the power block, power block efficiency, mass flow rate and the gross to net conversion factor based on the design point calculations.
- The next module is storage and currently it can design the two tank molten salt storage. It can able to compute the thermal power required for the storage, total mass and volume of the molten salt and also the dimensions of the tank.
- The next module in the design flow is receiver module. The scope of the master thesis mainly deals with the design method of the receiver module and so it will be discussed separately in the next section. The receiver design method can be able to calculate the dimensions of two types of tubular receiver: external and cavity receiver, tower height, mass flow rate, pressure drop and the thermal losses of receiver.
- The last module is the solar field which will design the solar field layout and the optical losses of the solar field.

## 4.3 Implementation Structure of Receiver Module in devISEcrs

As the *devISE<sub>crs</sub>* tool is written in Python, the receiver module is also implemented in Python. It is highly object oriented. The documentation of code is done using doxygen style. The structure of receiver design method implementation and the main functions are shown in the Figure 4.3.

The receiver module includes the design method for two types of receivers and it shares some design steps. So the inheritance structure is used to implement the two types of the receiver. The functionalities which are common to both receivers are placed in the receiver class and the two types of the receiver class are inherited from the receiver class. In each type of receiver class, there are two main functions design and efficiency. The design function which calls the other functions receiver geometry, receiver tube and panel, tower height and many sub functions to design and size the receiver. The efficiency function which calculates the receiver efficiency by calling several other losses function.

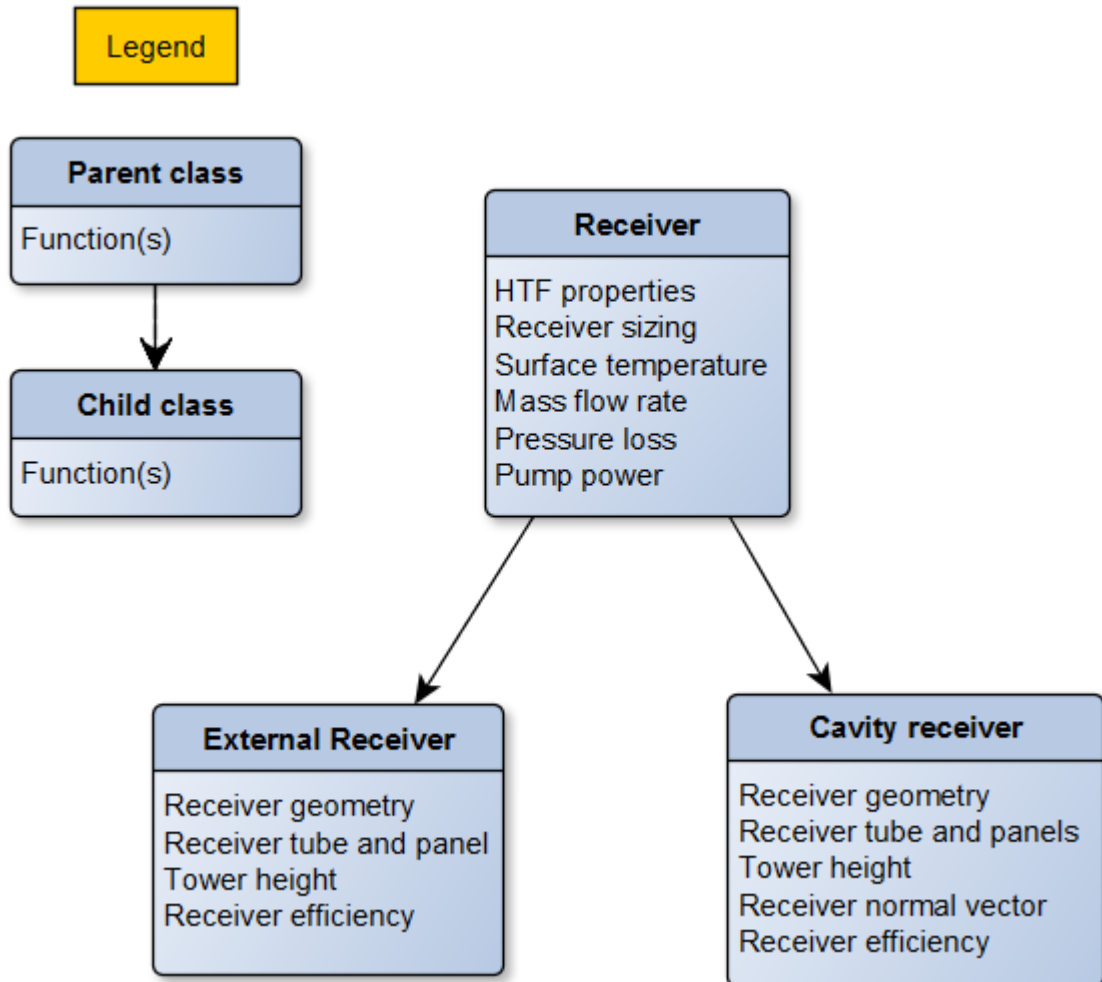


Figure 4.3: Class inheritance structure of the receiver module in devISEcrs

The receiver module needs the two main inputs from the power block and storage module to design the receiver which are thermal power required for the power block and the solar multiple. It is implemented in such a way that the other design parameters can either be given as an input parameter or can be calculated inside the receiver module. It can also be possible to call the particular function to perform specific design or to calculate only thermal losses for the existing receiver. The outputs from the receiver module is returned as a named tuple containing all the necessary parameters needed for the solar field module.

The current model allows the user to design with the receiver fluid molten salt and liquid sodium. The user can also specify the properties of any specific fluid and can be able to design the receiver. The other receiver fluids can also be incorporated in the model with ease.

The other parameters like design velocity of the receiver fluid, absorptivity of the coating, design wind velocity, inlet and outlet temperature of the receiver fluid and many other parameters are given default nominal value inside the receiver module. But all the parameters will be overwritten if the user specifies its value. The input and output parameters of the particular class and its default values are tabulated in the next section.

## 4.4 Inputs/outputs of Receiver Module

This section describes the input and output parameters of the receiver classes and also the used default values of some input parameters.

### 4.4.1 Receiver class

**Input parameters and its default values:**

Name	Default value	Unit
Thermal power required for power block	-	W
Solar multiple	-	-
Assumed receiver thermal efficiency	0.9	-
Temperature of hot fluid out	565	C
Temperature of cold fluid in	288	C
Ambient temperature	298	K
Absorptivity of the receiver surface	0.97	-
Velocity of the receiver fluid	4	m/s
Wind velocity	8	m/s
Emissivity of the receiver surface	0.88	-
Absolute viscosity of air	$1.846 \times 10^{-5}$	Kg/ms
Kinematic viscosity of air	$1.568 \times 10^{-5}$	$m^2/s$
Specific heat of air	1005	J/kgK
Volumetric expansion coefficient of air	$3.43 \times 10^{-3}$	1/K
Thermal conductivity of air	0.0257	W/mK
Thermal conductivity of receiver tube	23.9	W/mK
Efficiency of pump	0.8	-

Table 4.1: Input parameters and its default value of the receiver class

#### 4.4.2 External receiver class

##### Design input parameters and its default values:

These are the input parameters specific for external receivers.

Name	Default value	Unit
Heat transfer fluid	Molten salt	-
Receiver aspect ratio	1.5	-
Outer diameter of receiver tube	Diameter correlation	m
Thickness of receiver tube	0.002	m
Number of flow path	2	-
Tower height	Tower correlation	m

Table 4.2: Input parameters and its default value of the external receiver class

##### Output parameters:

Name	Unit
Area of the receiver	$m^2$
Height of the receiver	m
Diameter of the receiver	m
Outer diameter of receiver tube	m
Thickness of receiver tube	m
Number of panels	-
Number of tubes per panel	-
Tower height	m
Mass flow rate of the fluid	kg/s
Minimum allowable mass flow rate	kg/s
Incident receiver thermal power	W

Table 4.3: Output parameters of the external receiver class

#### 4.4.3 Cavity receiver class

##### **Input parameters and its default values:**

These are the input parameters specific for cavity receivers.

Name	Default value	Unit
Heat transfer fluid	Molten salt	-
Receiver aspect ratio	1	-
Cavity opening angle	180	<i>degrees</i>
Aperture to total height ratio	0.75	-
Aperture to total width ratio	1	-
Outer diameter of receiver tube	Diameter correlation	<i>m</i>
Thickness of receiver tube	0.002	<i>m</i>
Number of flow path	2	-
Cavity inclination angle	0	<i>degrees</i>
Tower height	Tower correlation	<i>m</i>
Tower Orientation	180	<i>degrees</i>

Table 4.4: Input parameters and its default value of the cavity receiver class

##### **Output parameters:**

Name	Unit
Area of the receiver	$m^2$
Total height of the receiver	$m$
Diameter of the receiver	$m$
Lip height	$m$
Outer diameter of receiver tube	$m$
Thickness of receiver tube	$m$
Number of panels	-
Number of tubes per panel	-
Cavity opening angle	<i>degrees</i>
Cavity inclination angle	<i>degrees</i>
Tower height	$m$
Mass flow rate of the fluid	$kg/s$
Minimum allowable mass flow rate	$kg/s$
Incident receiver thermal power	$W$
Receiver normal vector	-

Table 4.5: Output parameters of the cavity receiver class

# Chapter 5

## Results and Validation

This chapter explains about how the developed design method is validated and the results using that model is explained in the following sections.

### 5.1 Validation of the Design Method

The validation of design method is done using the reference plants. It is chosen in such a way that the reference plant is commercially well established and the data of the plant is available in the literature. Then the plant is designed using the developed model for the same specifications of the reference plant and it is compared against the reference plant to check the validity of the developed design method.

#### 5.1.1 External receiver

For the validation of external receiver, Gemasolar power plant in Spain is used as a test case. The developed design model is mainly aimed at molten salt receiver and so Gemasolar plant is the suitable test case. Gemasolar plant is the 20 MW solar tower power plant with 15 hours of storage located in the province of Seville, Spain. It is the first central tower plant with molten salt as a heat storage technology. The plant location and the characteristics are tabulated in the table 5.1.

#### Receiver design

The external receiver is designed using the model for the plant characteristics of Gemasolar and it is compared with the data available in the literature. 5.2 Receiver thermal losses

#### 5.1.2 Cavity receiver

5.1 Receiver design 5.2 Receiver thermal losses PS10 reference plant Table of plant characteristics data and location Table comparing design parameters comparison of receiver Validation of the receiver efficiency and thermal losses

Location	
Latitude	37.33
Longitude	5.19
Plant Characteristics	
Electric Power	19.9 MWe
Storage Capacity	15 hours
Receiver parameters	
Receiver thermal power	120 MWth
Receiver fluid	Molten salt
Tower height	140 m

Table 5.1: Gemasolar power plant characteristics

Design parameters	Gemasolar plant	devISEcrs model
Receiver diameter	8.1 m	7.4 m
Receiver height	10.6 m	11 m
Diameter of receiver tube	25 mm	21 mm
Thickness of receiver tube		1.2 mm
No. of receiver panels		12
No. of tubes per panel		92
Tower height	140 m	

Table 5.2: Comparison of Gemasolar receiver design parameters

## 5.2 Effect of Spillage Loss on Heliostat Size

# **Chapter 6**

# **Conclusions**

Write your conclusions here.

# Bibliography

- [1] Atacama solar tower project, Chile. [http://www.nrel.gov/csp/solarpaces/project\\_detail.cfm/projectID=3275](http://www.nrel.gov/csp/solarpaces/project_detail.cfm/projectID=3275). Accessed: 2016-06-28. 13
- [2] Concentrated solar power plant. [https://www.eeremultimedia.energy.gov/solar/graphics/concentrating\\_solar\\_power\\_tower\\_plant\\_illustration](https://www.eeremultimedia.energy.gov/solar/graphics/concentrating_solar_power_tower_plant_illustration). Accessed: 2016-06-22. vv, 8
- [3] Crescent dunes solar energy project, USA. [http://www.nrel.gov/csp/solarpaces/project\\_detail.cfm/projectID=60](http://www.nrel.gov/csp/solarpaces/project_detail.cfm/projectID=60). Accessed: 2016-06-28. 13
- [4] CSP power plant types. <http://www.solar-tower.org.uk/quick-start.php>. Accessed: 2016-06-21. vv, 3
- [5] Gemasolar power plant in spain. [http://www.torresolenergy.com/EPORTAL\\_IMGS/GENERAL/SENERV2/IMG2-cw4e41253840d81/gemasolar-plant-june2011-2b.jpg](http://www.torresolenergy.com/EPORTAL_IMGS/GENERAL/SENERV2/IMG2-cw4e41253840d81/gemasolar-plant-june2011-2b.jpg). Accessed: 2016-06-21. vv, 4
- [6] Solar irradiation types. <http://desktop.arcgis.com/en/arcmap/10.3/tools/spatial-analyst-toolbox/modeling-solar-radiation.htm>. Accessed: 2016-06-21. vv, 1
- [7] Solar receiver. <http://www.csp-world.com/news/20130402/00805/molten-salt-receiver-crescent-dunes-csp-plant-complete>. Accessed: 2016-06-22. vv, 5
- [8] Omar Behar, Abdallah Khellaf, and Kamal Mohammedi. A review of studies on central receiver solar thermal power plants. *Renewable and sustainable energy reviews*, 23:12–39, 2013. 2, 3
- [9] H Benoit, L Spreafico, D Gauthier, and G Flamant. Review of heat transfer fluids in tube-receivers used in concentrating solar thermal systems: Properties and heat transfer coefficients. *Renewable and Sustainable Energy Reviews*, 55:298–315, 2016. 25, 27
- [10] Nicholas Boerema, Graham Morrison, Robert Taylor, and Gary Rosengarten. Liquid sodium versus hitec as a heat transfer fluid in solar thermal central receiver systems. *Solar Energy*, 86(9):2293–2305, 2012. 9
- [11] Ch. Breyer and G. Knies. Global energy supply potential of concentrating solar power. In *Proceedings of SolarPACES 2009, Berlin, September 15–18, 2009*. 2
- [12] Yunus Cengel. Heat transfer a practical approach, mcgraw-hill korea. 2003. 17, 18, 19, 32
- [13] ZS Chang, X Li, C Xu, C Chang, and ZF Wang. The design and numerical study of a 2mwh molten salt thermocline tank. *Energy Procedia*, 69:779–789, 2015. 4

## BIBLIOGRAPHY

---

- [14] Joshua M Christian and Clifford K Ho. Cfd simulation and heat loss analysis of the solar two power tower receiver. In *ASME 2012 6th International Conference on Energy Sustainability collocated with the ASME 2012 10th International Conference on Fuel Cell Science, Engineering and Technology*, pages 227–235. American Society of Mechanical Engineers, 2012. 18
- [15] AM Clausing. An analysis of convective losses from cavity solar central receivers. *Solar Energy*, 27(4):295–300, 1981. 16
- [16] AM Clausing. Convective losses from cavity solar receiverscomparisons between analytical predictions and experimental results. *Journal of Solar Energy Engineering*, 105(1):29–33, 1983. 16, 21
- [17] AM Clausing, JM Waldvogel, and LD Lister. Natural convection from isothermal cubical cavities with a variety of side-facing apertures. *Journal of heat transfer*, 109(2):407–412, 1987. 22
- [18] Patricia Kuntz Falcone. A handbook for solar central receiver design. Technical report, Sandia National Labs., Livermore, CA (USA), 1986. iiiii, vv, vv, vv, vivi, 7, 8, 9, 10, 11, 12, 13, 14, 15, 25, 28, 29, 30, 32
- [19] Lukas Feierabend. *Thermal Model Development and Simulation of Cavity-Type Solar Central Receiver Systems*. 2010. vv, vv, vv, vv, 6, 15, 16, 21, 33
- [20] Austin Fleming, Charles Folsom, Heng Ban, and Zhiwen Ma. A general method to analyze the thermal performance of multi-cavity concentrating solar power receivers. *Solar Energy*, 2015. 6
- [21] Robert Flesch, Hannes Stadler, Ralf Uhlig, and Bernhard Hoffschmidt. On the influence of wind on cavity receivers for solar power towers: An experimental analysis. *Applied Thermal Engineering*, 87:724–735, 2015. vv, 16, 21
- [22] Charles W Forsberg. Developments in molten salt and liquid-salt-cooled reactors. In *Proceedings of the ICAPP*. Citeseer, 2006. 4
- [23] D Yogi Goswami and Frank Kreith. *Energy conversion*. CRC press, 2007. 5, 7
- [24] D Kearney, U Herrmann, P Nava, B Kelly, R Mahoney, J Pacheco, R Cable, N Potrovitz, D Blake, and H Price. Assessment of a molten salt heat transfer fluid in a parabolic trough solar field. *Journal of solar energy engineering*, 125(2):170–176, 2003. 4
- [25] JS Kraabel. An experimental investigation of the natural convection from a side-facing cubical cavity. In *Proceedings of the ASME JSME Thermal Engineering Joint Conference, Honolulu, HI, Mar*, pages 20–24, 1983. 16
- [26] Jesus M Lata and Monica Rodriguez, Manuel Alvarez de Lara. High flux central receivers of molten salts for the new generation of commercial stand-alone solar power plants. *Journal of Solar Energy Engineering*, 130(2):021002, 2008. iiiii, 6, 10, 13, 29
- [27] Zhirong Liao and Amir Faghri. Thermal analysis of a heat pipe solar central receiver for concentrated solar power tower. *Applied Thermal Engineering*, 102:952–960, 2016. 6
- [28] Zhirong Liao, Xin Li, Chao Xu, Chun Chang, and Zhifeng Wang. Allowable flux density on a solar central receiver. *Renewable Energy*, 62:747–753, 2014. 12, 25
- [29] Robert Y Ma. *Wind effects on convective heat loss from a cavity receiver for a parabolic concentrating solar collector*. Sandia National Laboratories, 1993. vv, 16, 21
- [30] M Prakash, SB Kedare, and JK Nayak. Investigations on heat losses from a solar cavity receiver. *Solar Energy*, 83(2):157–170, 2009. 21

- [31] MR Rodriguez-Sanchez, A Sanchez-Gonzalez, C Marugan-Cruz, and D Santana. New designs of molten-salt tubular-receiver for solar power tower. *Energy Procedia*, 49:504–513, 2014. 6
- [32] MR Rodriguez-Sanchez, A Sanchez-Gonzalez, C Marugan-Cruz, and D Santana. Flow patterns of external solar receivers. *Solar Energy*, 122:940–953, 2015. 14, 27
- [33] Marcelino Sanchez and Manuel Romero. Methodology for generation of heliostat field layout in central receiver systems based on yearly normalized energy surfaces. *Solar Energy*, 80(7):861–874, 2006. 5
- [34] MRI Sarker, Manabendra Saha, Md Sazan Rahman, and RA Beg. Recirculating metallic particles for the efficiency enhancement of concentrated solar receivers. *Renewable Energy*, 96:850–862, 2016. 6
- [35] FMF Siala and ME Elayeb. Mathematical formulation of a graphical method for a no-blocking heliostat field layout. *Renewable energy*, 23(1):77–92, 2001. 5
- [36] Dennis L Siebers and John S Kraabel. Estimating convective energy losses from solar central receivers. Technical report, Sandia National Labs., Livermore, CA (USA), 1984. vv, vivi, 6, 17, 18, 19, 21, 22, 32, 35
- [37] WB Stine. Power from the sun, published online by william b. stine and michael geyer, 2001. 1, 6, 29
- [38] William B Stine and Raymond W Harrigan. Solar energy fundamentals and design. 1985. 12, 16, 31
- [39] T Taumoefolau, Sawat Paitoonsurikarn, Graham Hughes, and Keith Lovegrove. Experimental investigation of natural convection heat loss from a model solar concentrator cavity receiver. *Journal of Solar Energy Engineering*, 126(2):801–807, 2004. 21
- [40] Soenke Holger Teichel. *Modeling and Calculation of Heat Transfer Relationship for Concentrated Solar Power Receivers*. 2011. vv, 17, 20, 22
- [41] Drake Tilley, Bruce Kelly, and Frank Burkholder. Baseload nitrate salt central receiver power plant design final report. Technical report, Abengoa Solar LLC, 2014. 17, 19, 29
- [42] F Trieb et al. Global concentrating solar power potentials, 2010. vv, 2
- [43] Michael J Wagner. *Simulation and predictive performance modeling of utility-scale central receiver system power plants*. University of Wisconsin -Madison, 2008. ii, vv, vv, vv, 7, 8, 11, 13, 14, 29
- [44] Min Wei, Yilin Fan, Lingai Luo, and Gilles Flamant. Design and optimization of baffled fluid distributor for realizing target flow distribution in a tubular solar receiver. *Energy*, 2016. 6
- [45] Al exis B Zavoico. Solar power tower design basis document. Technical report, Sandia National Labs., 2001. ii, vivi, 10, 13, 19, 25, 36

